COMPUTATIONAL FLUID DYNAMICS IN PANCREATICOBILIARY JUNCTION

Alim Turgaliyev, Doctor of Medicine

Submitted in fulfillment of the requirements for the degree of Master of Science in Biomedical Engineering

School of Engineering and Digital Sciences
Department of Chemical and Materials Engineering
Nazarbayev University

53 Kabanbay Batyr Avenue,
Astana, Kazakhstan, 010000

Supervisor: Yanwei Wang, Ph.D.
Co-supervisor: Zhandos Utegulov, Ph.D.

April 2024

DECLARATION

I hereby, declare that this manuscript, entitled “Computational fluid dynamics in pancreaticobiliary junction”, is the result of my work except for quotations and citations which have been duly acknowledged.

I also declare that, to the best of my knowledge and belief, it has not been previously or concurrently submitted, in whole or in part, for any other degree or diploma at Nazarbayev University or any other national or international institution.

Name: Alim Turgaliyev

Date: April 30th, 2024

Acknowledgments

It gives me great pleasure to thank everyone who made my thesis possible. I want to thank my supervisors, Prof. Yanwei Wang and Prof. Zhandos Utegulov, for their guidance and support throughout this research. I am grateful for teaching me the basics of fluid mechanics and computational fluid dynamics simulations.

I want to thank my colleagues from the Clinical Academic Department of Anesthesiology and Intensive Care at the University Medical Center for making my work schedule flexible and giving me more time to work on this thesis.

The author gratefully acknowledges the Laboratory of Computational Materials Science at the Center for Energy and Advanced Materials Science, National Laboratory Astana, for providing the essential computational resources required for this research.

Table of Contents

List of abbreviations

A	Cross-sectional area
B-P	Biliopancreatic type of junction
BPR	Biliopancreatic reflux

CD	Cystic duct
CBD	Common bile duct
CPBD	Common pancreaticobiliary duct
CHD	Common hepatic duct
CFD	Computational fluid dynamics
ERCP	Endoscopic retrograde cholangiopancreatography
HCPBD	High confluence of pancreaticobiliary ducts
PBD	Pancreaticobiliary ducts
PBM	Pancreaticobiliary maljunction
PBMWBD	Pancreaticobiliary maljunction without biliary dilatation
PBJ	Pancreaticobiliary junction
P-B	Pancreaticobiliary type of junction
PBS	Pancreaticobiliary system
PBR	Pancreaticobiliary reflux
PD	Pancreatic duct
V	V type of junction
Sc	Schmidt number
Q	Flow rate
Q_{GBe}	Gallbladder bile flow rate during emptying phase
Q_{GBa}	Gallbladder absorption rate
Q_{PD}	Pancreatic juice flow rate
Q_{CHD}	Hepatic bile flow rate

Q_{PBR}	Average flow rate across the half of the common bile duct
p	Pressure
P_{GBr}	Gallbladder bile pressure during refilling phase
P_{duo}	Pressure in duodenum

P_{inlet}	Pressure in inlet
P_{outlet}	Pressure in outlet
d	Diameter
a	Power index
m	Papanastasiou parameter
$\dot{\gamma}$	Shear rate
τ_0	Yield stress
L	Length
n_b	Number of buffles
ξ_b	Baffle height ratio
h_b	Thickness of baffles
Δ��	Distance between two successive baffles
RSO	In region of sphincter Oddi
Re	Reynolds number
μ	Dynamic viscosity
μ_0	Zero shear rate viscosity
μ_∞	Infinite shear rate viscosity
μ_{∞}	Plastic viscosity
λ	Time constant
ρ	Density
p_0	Threshold pressure
Π_0	Prescribed pressure

π	Pi value
u	Flow velocity
u	Velocity vector

D	Mass diffusivity
F	Volume force vector
K	Viscous stress tensor
I	Identity matrix
n	Unit normal vector
∇	Vector differential operator
T	Temperature
V_0	Flow rate
D_z	Entrance/exit thickness
S	Strain-rate tensor
Ωout	Domain's outlet

Ωin Domain's inlet

List of tables

List of figures

Abstract

Pancreaticobiliary maljunction without biliary dilation is associated with pancreaticobiliary reflux, a pathophysiologic factor underlying a wide range of diseases, including gallbladder cancer. This work used computational flow simulations to examine the mechanisms and relevant geometric features that influence pancreaticobiliary reflux and assess the impact of surgical interventions.

The results suggest that the refilling phase is the primary mechanism driving pancreaticobiliary reflux. Moreover, the cystic duct diameter was the most critical factor determining the reflux dynamics. Furthermore, the configuration of the baffle system (the baffle height ratio and the number of baffles) affected the dynamics of pancreaticobiliary reflux.

Also, the study underscores the potential therapeutic efficacy of cholecystectomy and

endoscopic retrograde cholangiopancreatography in managing pancreaticobiliary reflux in cases of pancreaticobiliary maljunction without biliary dilatation. These interventions offer promising avenues for reducing reflux-related complications and mitigating the progression of associated diseases.

Chapter 1 - Introduction and literature review

1.1. Pancreaticobiliary system

The pancreaticobiliary system (PBS) is the network of organs and ducts in the abdomen cavity involved in the secretion and transport of bile and pancreatic juices to the duodenum to facilitate the digestion and absorption of nutrients from food. The system comprises the pancreas, liver, gallbladder, sphincter Oddi, and ducts.

Hepatocytes inside the liver produce the aqueous solution called bile into the system of tiny tubes called intrahepatic biliary ducts (Boyer, 2013). Intrahepatic biliary ducts end with right and left hepatic ducts that form a common hepatic duct (CHD) outside the liver (Zyromski, 2015). CHD ends when it combines with a cystic duct (CD) and forms a common bile duct (CBD).

CD is the connection between the gallbladder that stores and concentrates bile and the other extrahepatic ducts (Li, 2021). The cystic duct structure can have folds called Heister's valves (Li, 2021). Although Heister, in the 18th century, named the spiralling features of cystic ducts "valves," the valvular function of these features is doubted (Li et al., 2007).

Figure 1

Schematic sketch of the pancreaticobiliary system in PBMWBD (B-P type of junction)

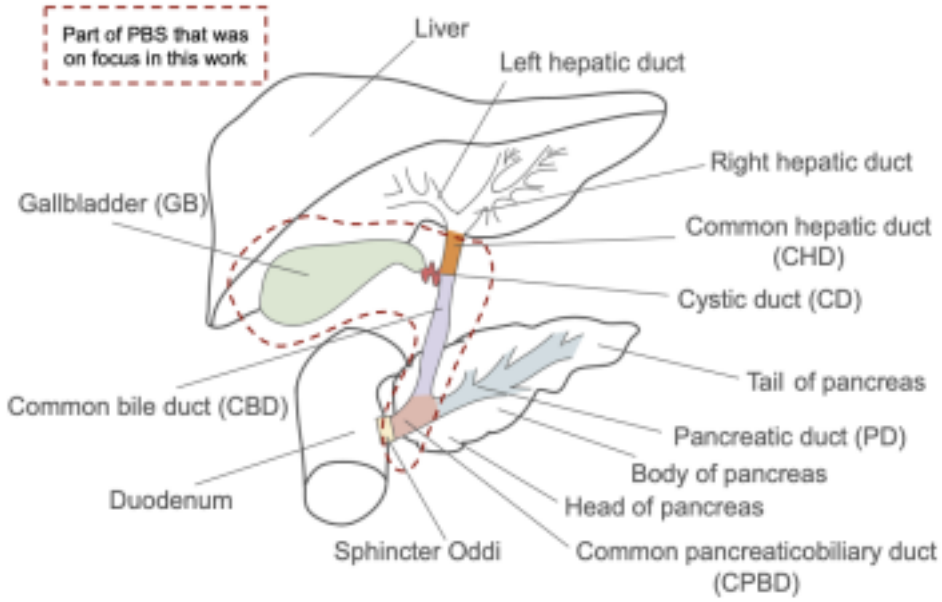

CBD ends in a duodenum wall, usually forming with the main pancreatic duct (PD), which flows pancreatic juice from the pancreas, a common pancreaticobiliary duct (CPBD) that is surrounded by the muscle called sphincter Oddi, which regulates the flow of juices to

the duodenum and prevents the refluxes between these two biofluid systems. Papilla of Vater is a small nipple-like structure located in the duodenum in which the PBS fluids drain.

1.2. Pancreaticobiliary maljunction

In certain instances, the pancreaticobiliary junction (PBJ) may deviate from its typical location to outside the sphincter of Oddi due to a congenital anomaly known as pancreaticobiliary maljunction (PBM) (Ono et al., 2020).

Arnolds (1906) was the first who reported PBM based on the German autopsy case. Ono et al. (2020) stated that there is a significantly higher incidence of PBM in Asian populations compared to other parts of the world. Unfortunately, the prevalence of PBM within Kazakhstan remains undetermined.

According to Fukuzawa et al. (2020), PBM manifests in two forms: PBM with dilated biliary duct and PBM without biliary dilatation (PBMWBD). Figure 1 provides a schematic representation of the pancreaticobiliary system in PBMWBD.

In a study conducted by Morine et al. (2013), data was collected from 141 institutions across Japan from 1990 to 2007 to determine the prevalence of PBM. The study's results showed a significant difference in the frequency of PBM with dilated biliary duct compared to

PBMWBD. In the paediatric group, PBM with a dilated biliary duct was overwhelmingly more common, accounting for 93.3% of cases, whereas only 6.7% were identified with PBMWBD. A PBM with dilated biliary duct in the adult demographic represented 66% of cases, while PBMWBD accounted for 34%. The authors stated that PBMWBD was usually identified in adulthood due to less frequent symptoms such as abdominal pain in childhood.

Kaneko et al. (2007) found that symptoms of PBM, such as abdominal pain, occur due to increased pressure in the pancreaticobiliary system caused by the formation of a protein plug. The authors noted that these plugs are mostly made up of lithostathine, a part of pancreatic juice, and can dissolve spontaneously. This temporary nature of symptoms is responsible for the underdiagnosis of PBMWBD.

Pancreaticobiliary maljunction is a condition that is closely associated with pancreaticobiliary reflux (PBR), which is a significant contributor to the development of various diseases. PBR can lead to gallbladder cancer, gallbladder polyps, gallstones, acute and chronic cholecystitis (Da et al., 2024). According to Morine et al. (2013), gallstones were present in 24% of PBMWBD cases, while biliary tract cancers were found in 42.4% of cases of PBMWBD, with 7.3% being bile duct cancer, and 88.1% being gallbladder cancer, and 4.6% being other cancers. Kamisawa et al. (2012) suggest that the continuous presence of

pancreatic juice reflux in the bile duct can damage the biliary tract epithelium, leading to cancer development.

It's worth noting that PBR can also occur in anatomically normal PBJ under specific circumstances, such as when the length of the common pancreaticobiliary duct exceeds 6 mm. This condition is called high confluence of pancreaticobiliary ducts (HCPBD), which is considered as an intermediate variant of PBM (Kamisawa et al., 2002).

Treatment strategies for PBMWBD are still controversial (Fukuzawa et al., 2020), so doctors need to better understand the mechanism of the PBR to choose the best treatment option for patients.

Several studies have found the mechanism underlying pancreaticobiliary reflux in PBMWBD. Fukuzawa et al. (2020) conducted a mechanical experiment to study PBR in that they used several infusion and syringe pumps, infusion sets and silicone tubes to simulate PBS. Tajikawa et al. (2023) formulated a mathematical 1D model of PBMWBD to explore PBR under different sphincter Oddi type motions. Both investigations suggest that the refilling phase of the gallbladder has a primary role in PBR, suggesting that removing the

gallbladder could serve as an effective therapeutic strategy.

However, these studies have some limitations. Both experiments used simple models that failed to account for anatomical features of the pancreaticobiliary system. For instance, the presence of Heister valves, which could potentially protect against reflux, must be accounted for. The variation in the PBJ type and CPBD length was also not considered in the studies. Anatomical features could influence the dynamics of PBR, potentially confounding the conclusions drawn from these experiments.

Also, these studies did not simulate or discuss endoscopic retrograde cholangiopancreatography (ERCP) interventions as a treatment option for PBMWBD. According to Qian et al. (2023), ERCP can relieve symptoms and be a bridge to radical surgery for patients with PBMWBD.

1.3. Computational fluid dynamics in pancreaticobiliary system

Computational fluid dynamics (CFD) has been applied to the pancreaticobiliary system for many years, but all these studies focused more on the pancreaticobiliary system's biliary part (Tajikawa et al., 2023).

Ooi et al. (2003) used fluid-structure interaction simulation in a 2D model of the cystic duct to investigate deformation of cystic duct. They demonstrated that the centre part will experience the most tube deformation.

Ooi et al. (2004) conducted a study to examine the impact of geometry on idealised 2D and 3D models of the cystic duct. The results showed that the height and number of baffles have a more significant impact on resistance than the curvature of the cystic duct and the angle between the neck and the gallbladder. Also, they found that flow data from the idealised model aligned with data from realistic models obtained from operative cholangiograms of two patients.

Li et al. (2007) created rigid and elastic 1D models of the human biliary system to estimate pressure drop during refilling and emptying phases for Newtonian fluid. According to the authors, high pressure drop during the emptying phase could lead to stasis bile in gallbladder. They found that the pressure drop can rise by 4.3% for every 1% reduction in cystic duct diameter. The authors added that the rigid model provides a similar to elastic model estimation if the duct wall's Young's modulus is more than 400 Pa.

Li et al. (2008) extended their previous work by implementing Non-newtonian flow.

The findings demonstrated that elastic deformation of the cystic duct and non-Newtonian bile increase the resistance of the cystic duct.

Al-Atabi et al. (2012) used computational fluid simulation in a 3D model of a real cystic duct. The results showed that strong secondary flow caused by the ducts' curvature led to four times more significant pressure drop than a straight, circular tube with an equivalent length and diameter. The authors highlighted that the cystic duct works as a passive resistor.

Kuchumov et al. (2014) simulate flow in a 3D model of PBS. Although the authors include the pancreatic part, they mistakenly simulate PBM while stating that the model represents a typical case. The description of their model lacks comprehensive details, such as the flow rate of pancreatic juice and the diameter of the pancreatic duct. Furthermore, the authors stated nothing about the presence of refluxes within the system.

Meyer et al. (2017) created a 3D model of bile flow inside the liver lobe that can predict velocity and pressure inside the liver lobe. They validate their model by in-vivo experiments on rats. The authors stated that their model can be used to quantify biliary flow after drug-induced liver injury.

Kuchumov et al. (2017) investigated the peristaltic flow within the papilla of Vater, identifying a condition at which reflux between the duodenum and CPBD is possible. Additionally, they offer insights about optimising the channel shape through catheterization to restore normal flow.

Kuchumov (2019) and Kuchumov et al. (2020) studied flow in the patient-specific models of PBS obtained from imaging techniques (MRI, ultrasounds). They showed that

patient-specific flow simulation can give surgeons tools for predicting surgery outcomes. However, the pancreatic part of PBS was not included in their models.

Baghaei et al. (2020) explored bile flow dynamics in bile ducts obstructed by gallstones using fluid structure interaction in a 2D system. The study reveals that in scenarios of partial obstruction of the bile ducts, there are no significant alterations in pressure

Although CFD was used for investigation of flow in PBS for many years this method was not applied to investigate the refluxes between biliary and pancreatic parts.

1.4. Aim and objectives

This study will be the first to investigate the pancreaticobiliary system using computational flow simulations to determine the mechanism and features that affect PBR in

PBMWBD and evaluate the effect of surgical procedures.

Objectives of the study:

1. to develop a 2D model of PBMWBD.
2. to evaluate the mechanism and anatomical and fluid features that affect PBR in a 2D model of PBMWBD.
3. to evaluate the effect of surgical procedures on PBR in a 2D model of PBMWBD.

Chapter 2 - Development of 2D idealised model of pancreaticobiliary maljunction without biliary dilatation

The developed model was based on scientific data about the pancreaticobiliary system. The model parameters are presented in Table 1. The geometry of the model was created to be similar to previously published CFD studies (Ooi et al., 2004; Li et al., 2007; Li et al., 2008) with the addition of the PBJ part.

Table 1

Model parameters

Part of system	**Parameter Value**
Common hepatic duct (CHD)	Diameter (d_{CHD}) 6 mm
	Length (L_{CHD}) 40 mm Hepatic bile flow rate (Q_{CHD}) 0.5 mL/min
Cystic duct (CD) and gallbladder	Cystic duct diameter (d_{CD}) 3.5 mm
	Cystic duct length (L_{CD}) 40 mm
	Number of buffles (n_b) 9
	Baffle height ratio ($_b\xi$) 0.5
	Thickness of baffles (h_b) 0.5 mm Distance between two successive baffles $(\Delta\square\square)^{\Delta\square\square} =^{\square\square}{}_{\blacklozenge\blacklozenge\blacklozenge\blacklozenge}-\square\square_{\blacklozenge\blacklozenge}h_{\blacklozenge\blacklozenge}\square\square_{\blacklozenge\blacklozenge}-1$
	Gallbladder bile flow rate during emptying phase (Q_{GBe}) 0.83 mL/min

	Gallbladder pressure during refilling phase (P_{GBr}) = P_{duo}
	Gallbladder diameter (d_{GB}) 30 mm
	Gallbladder absorption rate (Q_{GBa}) 23 mL/h
Common bile duct (CBD)	Diameter (d_{CBD}) 6 mm
	Length (L_{CBD}) 100 mm
Pancreaticobiliary	Type B-P

junction (PBJ)	Length of common pancreaticobiliary duct (L_{CPBD}) 4.5 mm
	Diameter of CPBD (d_{CPBD}) d_{PD} or d_{CBD} (based on type of PBJ)
	Length of CPBD in region of sphincter Oddi ($L_{CPBD-RSO}$) = wall thickness of duodenum 1.6 mm
	Diameter of CPBD in region of sphincter Oddi, when it relaxed ($d_{CPBD-RSO}$) 0.3 mm
	Pressure in duodenum (P_{duo}) 0 mmHg
	Diameter of pancreatic duct (d_{PD}) 3 mm
	Pancreatic juice flow rate (Q_{PD}) 1 mL/min
Fluid	Density (ρ) 1010 kg/m^3
Flow	Dynamic viscosity (μ) 1 mPa × s Inlets during gallbladder phases Stationary: $Q_{CHD,}$ Q_{PD} Emptying: $Q_{CHD,}$ $Q_{PD,}$ Q_{GBe} Refilling: $Q_{CHD,}$ Q_{PD} Outlets during gallbladder phases Stationary: Q_{GBa}, P_{duo} Emptying: P_{duo} Refilling: P_{GBr}, P_{duo}

2.1. Geometry

The length and width of the extrahepatic bile ducts (CHD and CBD) are around 100–150 mm and 5-15 mm, respectively, with the L_{CHD} is approximately 40 mm (Dodds et al. 1989, as cited in Li, 2021). Our model adopts a uniform diameter for both the CHD and CBD, set at 6 mm, and L_{CBD} and L_{CHD} are set at 10 cm and 4 cm, respectively, consistent with the parameters used in Li et al. (2008).

The cystic duct exhibits varying dimensions. Ooi et al. (2004) reported a length (L_{CD}) range of 10 to 60 mm and a diameter (d_{CD}) range of 2 to 5 mm. Dodds et al. (1989, as cited in Li, 2021) stated that L_{CD} is about 35 mm long and d_{CD} is 3 mm wide. Garg et al. (2022) examined 100 MRI images, observing that differences in length and diameter between gallstone and non-gallstone cases were not statistically significant. In gallstone patients, L_{CD}

measured 22 ± 8 mm, and d_{CD} measured 3.29 ± 1.49 mm, while in non-gallstone patients, it measured 19 ± 8 mm in length and 2.8 ± 0.87 mm in diameter. Our model standardised L_{CD} to 40 mm, aligning with previous computational fluid dynamics studies (Ooi et al., 2004; Li et al., 2007; Li et al., 2008). d_{CD} was set to 3.5 mm, representing the median value within the physiological range.

The CD may feature folds (Heister valves, baffles), which can significantly increase flow resistance or pressure drop (Li, 2021). Instances of more than 18 baffles in a human cystic duct are relatively rare (Li et al., 2007), while the number of folds can range from two to fourteen (Ooi et al., 2004). In our modelling, we set the number of baffles (n_b) to 9, representing the midpoint within the physiological range of 0 to 18.

The baffle height ratio (ξ_b) is the ratio of baffle height to the channel diameter. Research by Ooi et al. (2004) based on operative cholangiograms indicates that ξ_b typically ranges from 0.2 to 0.6. Li et al. (2007) and Li et al. (2008) utilised ξ_b values between 0.3 and 0.7 in their studies. In our 2D model, we set ξ_b to 0.5, which falls within the overlapping ranges suggested by both research sets.

The thickness of baffles (h_b) in our study aligns with the data of Li et al. (2007) and Li et al. (2008), and was set at 0.5 mm.

Distance between two successive baffles (Δ) in our study was determined using the formula outlined in Li et al. (2007): $\Delta = \frac{L - n_b h_b}{n_b - 1}$

Figure 2A shows a schematic representation of the cystic duct with the geometric parameters discussed above. The height of the baffles is determined by multiplying the baffle

height ratio by the cystic duct diameter.

The diameter of the pancreatic duct (the Wirsung duct) exhibits distinct variations across different pancreas regions. Typically, its diameter measures around 3 mm in the pancreatic head and 2 mm in the body and 1 mm in the pancreatic tail (Möller et al., 2023). The junction between the pancreatic duct and the common bile duct usually occurs in the pancreatic head, so d_{PD} was established at 3 mm.

Because the accessory pancreatic duct (the Santorini duct) does not have a connection to the bile system, it was excluded from our model. Our model operates under the assumption that all pancreatic fluid drains through the main pancreatic duct.

As delineated by Sherifi et al. (2018), the junction between the pancreatic duct and the common bile duct can be categorised into three types: V type, B-P type, and P-B type. In Figure 2B, we observe a representation of the B-P type junction, wherein the common bile

Figure 2

Schematic sketch of the model geometry

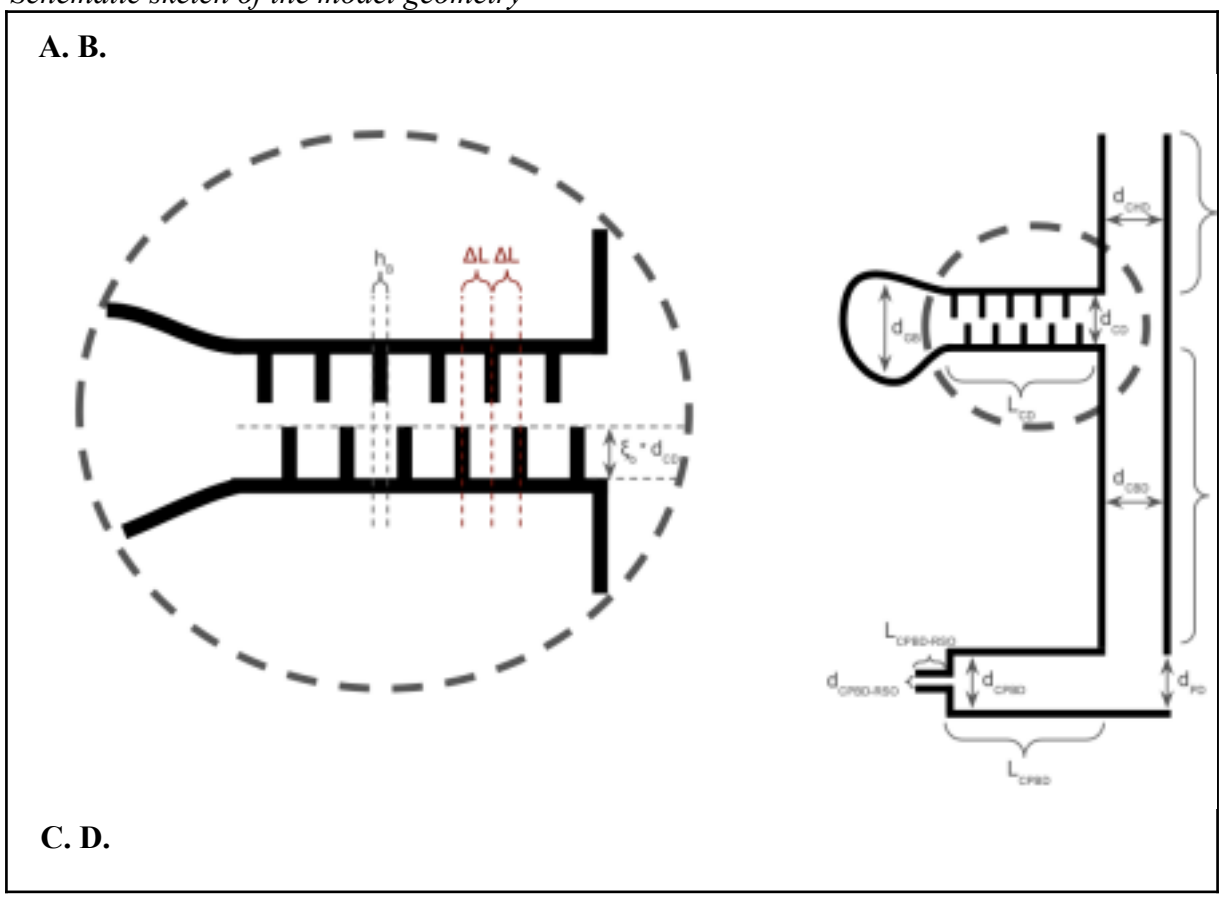

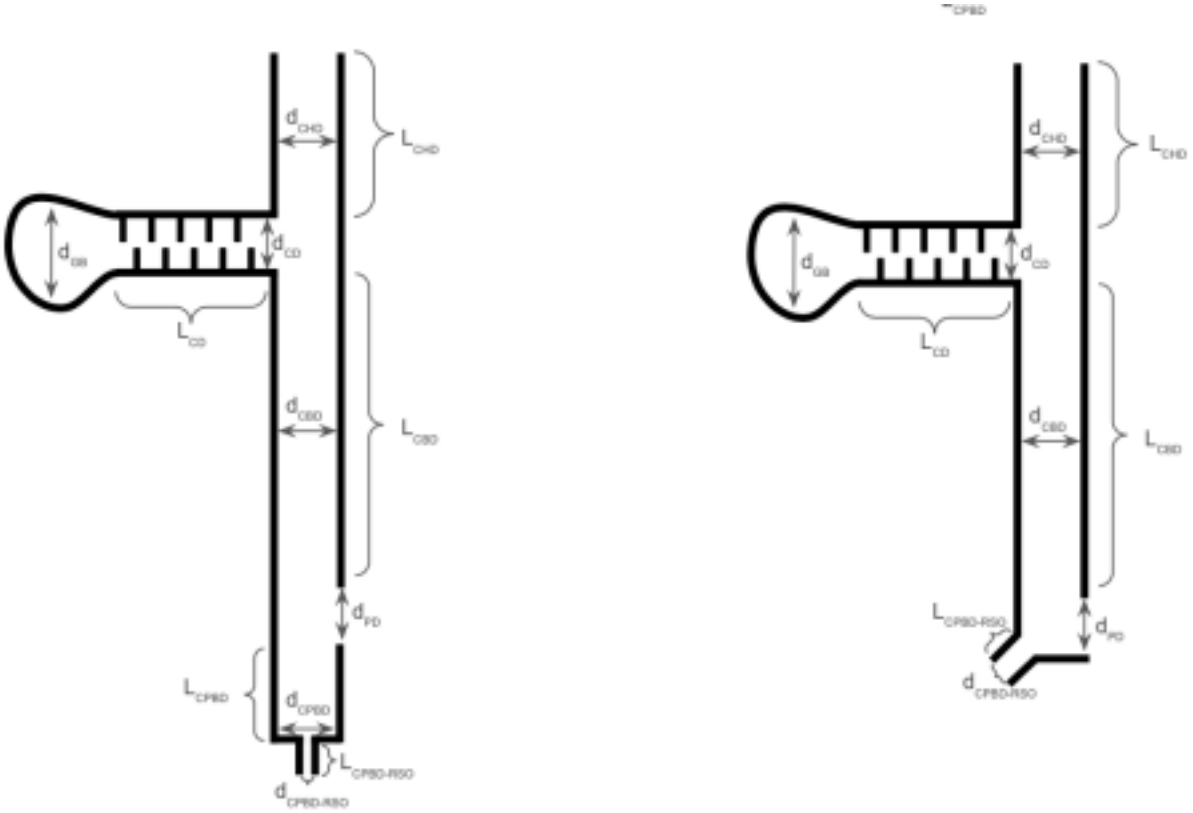

Note. A. Cystic Duct, B. B-P type, C. P-B type, D. V type.

duct empties into the pancreatic duct, resulting in the formation of CPBD. Figure 2C illustrates the reverse scenario, where the pancreatic duct drains into the CBD, leading to the creation of CPBD. Figure 2D shows the V type of junction, characterised by the direct contact of the pancreatic duct and biliary duct without the formation of a common pancreaticobiliary duct. Our model type was set to B-P because Sherifi et al. (2018), after examining 63 magnetic resonance cholangiopancreatography images, stated that it is the most common type of union.

In individuals without pathological conditions, the common pancreaticobiliary duct typically ranges from 1 to 12 mm in length, with an average measurement of 4.5 mm, as reported by Misra and Dwivedi (1990). Therefore, in our modelling framework, the length of the common pancreaticobiliary duct (L_{CPBD}) was established at 4.5 mm to align with this observed mean value.

No data was found regarding the length of CPBD in the sphincter region of Oddi. Therefore, we assume that the length of the common pancreaticobiliary duct at the region of the sphincter of Oddi ($L_{CPBD\text{-}RSO}$) is equivalent to the wall thickness of the duodenum. According to Nylund et al. (2012), the duodenal wall thickness is 1.6 mm.

Sphincter Oddi exhibits repeated contraction and relaxation that causes a change in diameter of ducts under the sphincter Oddi. Tajikawa et al. (2023) assumed that the inner

diameter of the contracted CPBD in the region of sphincter Oddi in relaxed state is 0.3 mm because during ERCP physicians put guidewire, that have diameter of 0.6-0.8 mm, with slight friction into the papilla of Vater. This is a reason why in our model $d_{CPBD\text{-}RSO}$ was set to 0.3 mm.

2.2. Fluid

The pancreaticobiliary system has two types of biofluids: bile and pancreatic juice. However, the properties of gallbladder bile, such as viscosity, diverge from those of hepatic (or duct) bile due to absorption processes within the gallbladder, leading the pancreaticobiliary system to be a three-fluid system.

The rheological characteristics of PBS fluids vary significantly, exhibiting both Newtonian and non-Newtonian behaviours, with their viscosity being influenced by various factors including diet, diseases and pharmacological treatments. A compilation of studies exploring the dynamic viscosity of PBS fluids can be found in Appendix Table 1. While traditionally, bile was classified as a Newtonian fluid subsequent research has established its non-Newtonian nature (e.g., Coene et al., 1994; Jungst et al., 2001). However, a limited

number of studies has been done about pancreatic juice viscosity and its potential non-Newtonian behaviour is unclear. Usually pancreatic juice is considered as a Newtonian fluid.

For simplicity reasons, in our work we used a one-fluid model with dynamic viscosity equal to 1 mPa × s that has Newtonian behaviour.

The density of bile and pancreatic juices is quite similar. Bile densities range from 965.9 to 1014.5 kg/m^3(Li et al., 2008) and from 1003 to 1013 kg/m^3(Saida, 1992). Pancreatic juice density is 1010 kg/m^3(Tajikawa et al., 2023). So, in our model, we used a density (ρ) equal to 1010 kg/m^3.

2.3. Flow

The flow directions in PBS change with the phases of gallbladder (Figure 3). Fukuzawa et al. (2020) delineated phases of the gallbladder as follows: refilling, stationary and emptying phases.

During the refilling phase (Figure 3A) that starts after the end of the emptying phase, the pressure inside the gallbladder (P_{GBr}) becomes equal to the pressure in the duodenum (Tajikawa et al., 2023). Given that the duodenal pressure (P_{duo}) serves as the baseline pressure

for pancreaticobiliary flow, we adopt the assumption used by Tajikawa et al. (2023) that $P_{duo}$is equal to the intraperitoneal and atmospheric pressures, thereby considered to be 0 mmHg.

During the stationary phase (Figure 3B), the gallbladder is in a state when it is not contracting or expanding. However, due to continuous absorption processes in the gallbladder, bile steadily flows into the gallbladder (Fukuzawa et al., 2020). Fukuzawa et al. (2020) suggest that under normal dietary habits, individuals typically consume three meals a day, resulting in gallbladder emptying occurring approximately every 8 hours. During each contraction, it is assumed that 80 percent of the gallbladder's maximal capacity is flow out, equating to 40 mL per hour. Consequently, within the seven-hour interval following a contraction, the gallbladder should be filled at least by 40 mL of bile. Considering that gallbladder bile exhibits a significantly higher concentration of bile acids (5–20 times greater) than hepatic bile, Fukuzawa et al. (2020) propose that the rate of bile flow into the gallbladder during the stationary phase is five times greater than the minimal value, approximating 200 ml (40 mL× 5) per 7h. Therefore Fukuzawa et al. (2020) suggest that absorption rate in gallbladder (Q_{GBa}) during stationary phase is 23 mL/h. The calculation was as follows: [(200 mL - 40 mL] / 7h. In our model we used this assumption.

Figure 3
Schematic flow directions during gallbladder phases

A. Refilling phase **B.** Stationary phase,

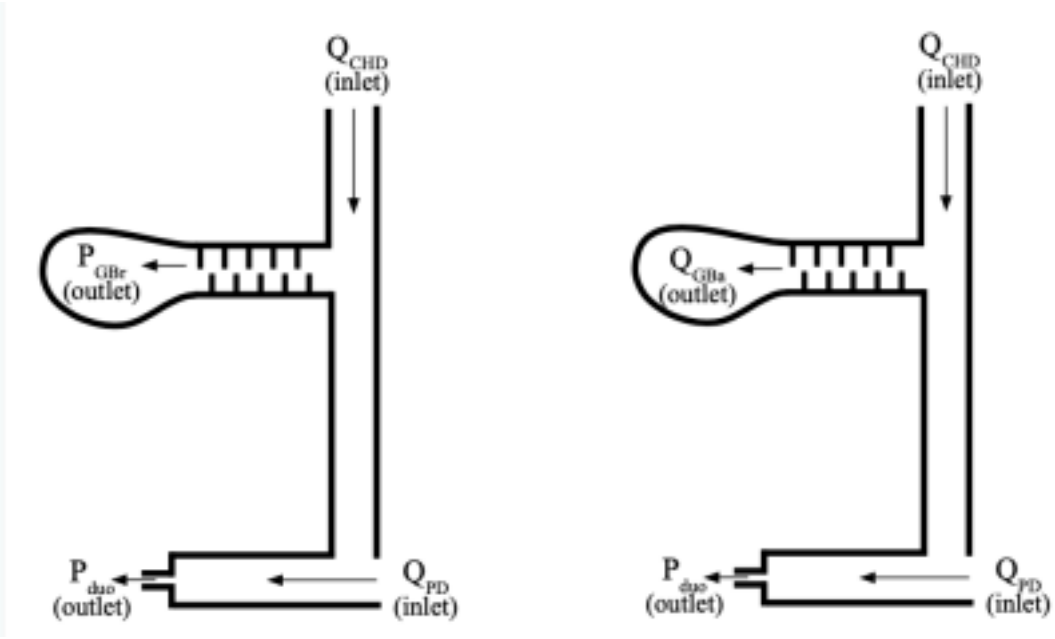

C. Emptying phase

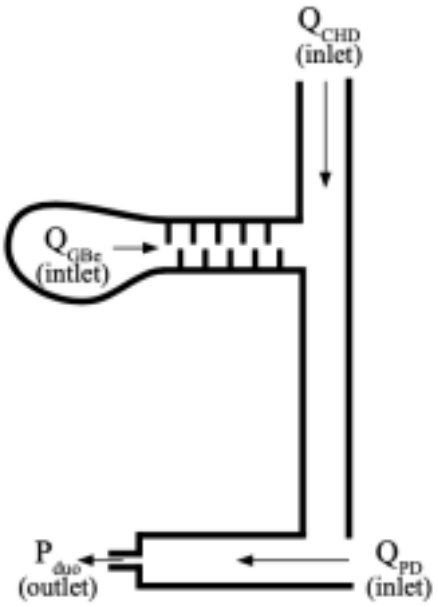

Emptying phase (Figure 3C) characterised by contraction of the gallbladder muscles, that prompts the removal of bile from the gallbladder (Housset et al., 2016). Howard et al. (1991) in ultrasound study estimated that after the meal gallbladder bile flow rate (Q_{GBe}) is equal to 0.84 mL/min (± 0.34 mL/min). In our work we used Q_{GBe} equal to this mean value. The baseline flow rates from the pancreas (Q_{pd}) and liver (Q_{CHD}) were determined by

Fukuzawa et al. (2020), who used approximation that the pancreas produces 1000-1500 mL of

pancreatic juice and the liver produces 700 mL of bile per day. In line with this approach, we utilised similar values for Q_{pd} and Q_{CHD} as Fukuzawa et al. (2020), equating to 1 mL/min and 0.5 mL/min, respectively.

Using the assumption with a one-fluid model and dimensions of the model, we can calculate that flow in our system will be laminar based on Reynolds number ($Re = \frac{\rho u d}{\mu}$, where d is the diameter of the duct in m, and u is the mean velocity of the fluid in m/s). Also, the hydrodynamic theory states that viscous resistance is significantly larger than the inertia of flow and that the curvature of the ducts has no effect on the flow since its Re is small enough.

Tajikawa et al. (2023) calculate that based on the Schmidt number ($Sc = \frac{\mu}{\rho D}$, where D is the mass diffusivity in m^2/s), the mass transfer in PBS is mainly caused by the bulk motion of a fluid. Furthermore, the authors compute the duct's compliance and claim that the dilatation caused by a change in pressure may be disregarded. Therefore, pancreaticobiliary ducts were represented as rigid, straight pipes in our work.

Laminar flow in PBS can be described in Navier-Stokes equations:

Conservation of momentum: $\rho(\mathbf{u}\nabla)\mathbf{u} = \nabla[-p\mathbf{I}+\mathbf{K}] + \mathbf{F}$

Conservation of mass: $\rho\nabla\mathbf{u} = 0$

where ∇ is the a vector differential operator, p is pressure (Pa), **F** is the volume force vector (N/m^3), **u** is the velocity vector (m/s), **K** is the viscous stress tensor (Pa) = $\mu[\nabla\mathbf{u}+(\nabla\mathbf{u})^T]$, T is absolute temperature (K), **I** is the identity matrix.

In our model, we incorporated two distinct types of outlet conditions. The first type is pressure outlet: $[-p\mathbf{I}+\mathbf{K}]n = -p_0\mathbf{n}$, $p_0 \leq p_0$, where **n** is a unit normal vector representing the direction in which the force is acting. This outlet type was employed to simulate the conditions at P_{duo} and P_{GBr}, both of which were assigned a value of 0 mmHg.

The second type is characterised as a fully developed flow outlet, governed by the equation $\mathbf{ut} = 0$, $P_{outlet}: V_0 = -\int_{\partial\Omega out} D_z\mathbf{u} \cdot \mathbf{n}dS$, where V_0 - flow rate (m^3/s), D_z - exit/entrance thickness (m), Ωout - domain's outlet, S - the strain-rate tensor (= ½ [∇ + (∇)]). This type of outlet was used to describe Q_{GBa} during the stationary phase. For this scenario, Dz was set equal to the width of the gallbladder (30 mm).

All inlets (Q_{GBe}, Q_{CHD}, Q_{PD}), in developed model was fully developed flow inlets: $\mathbf{ut} = 0$, $P_{inlet}: V_0 = -\int_{\partial\Omega in} D_z\mathbf{u} \cdot \mathbf{n}dS$, where Ωin - domain's inlet. Dz in inlets was set to the diameter of related ducts.

The simulation of flow in PBS was created using Comsol Multiphysics® 6.2 as a laminar

non-compressible flow with a nonlinear stationery solver (tolerance = 0.001) without slip at walls. Physics-Controlled mesh with normal element size was used for simulations.

2.4. Discussion

While our model offers a comprehensive 2D idealised representation of pancreaticobiliary maljunction without biliary dilatation, it is important to acknowledge its limitations and avenues for enhancement.

Our model has certain limitations. Firstly, it does not incorporate the phasic contraction of the sphincter Oddi. Instead, we relied on an assumption derived from Tajikawa et al. (2023) that the inner diameter of the CPBD in the region of sphincter Oddi, under basal pressure, is equal to 0.3 mm. While this assumption provides a baseline, it may not fully capture the dynamic nature of the sphincter Oddi function.

Secondly, a stationary solver that is used in our simulations represents another limitation. While suitable for simulating refilling and stationary phases of the gallbladder, typically 4-10 hours, it may not be the optimal choice for simulating the rapid emptying phase, which occurs within 30 minutes. A time-dependent solver seems to be more suitable during this phase.

The third limitation of our model is that the hepatic flow rate (Q_{CHD}) and pancreatic flow rate (Q_{PD}) are based on assumptions from Fukuzawa et al. (2020). However, it's important to note that flow rates can vary among patients, which may affect the accuracy of our model.

There are several avenues for enhancement. The first potential enhancement could involve the implementation of a three-fluid model flow, which would offer a more realistic simulation of pancreaticobiliary flow dynamics within PBS.

The second potential enhancement is that the model could be reconfigured to encompass a broader spectrum of pancreaticobiliary pathologies, such as stenotic and dilated types of PBM, as well as HCPBD.

Additionally, integrating patient-specific 3D models obtained from magnetic resonance cholangiopancreatography scans in CFD simulations could be used as a part of personalised medicine.

The fourth potential enhancement could be exploring various flow rates within the pancreatic and hepatic inlets. This approach could not only assess PBR but also allows the investigation of biliopancreatic reflux (BPR) phenomena. Moreover, the study of BPR could

benefit from examining the emptying phase during different configurations of the union between the cystic duct and the common bile duct. Such investigations hold particular significance given the role of BPR in the pathogenesis of pancreatitis and the development of pancreatic and periampullary cancers (Muraki et al., 2020).

By incorporating these enhancements and modifications, future models would be better equipped to address a broader range of research questions and clinical scenarios, thereby advancing our understanding of pancreaticobiliary fluid dynamics and improving patient care strategies.

Chapter 3 – Mechanism and influencing factors of pancreatic juice reflux in pancreaticobiliary maljunction without biliary dilatation

3.1. Mechanism of reflux

This CFD study aims to investigate the mechanism underlying PBR by employing computational fluid dynamics simulations. Utilising the model described in Table 1, we investigate the flow patterns during different phases of gallbladder activity - stationary, emptying, and refilling.

During the stationary phase, no pancreaticobiliary reflux was observed. Figure 4A-C shows the velocity magnitude, pressure, and streamline distribution during the stationary phase. It is observed that bile flows from the common hepatic duct and reaches a T-junction, where the flow divides. One stream proceeds to the cystic duct and subsequently into the gallbladder. At the same time, the other stream continues to the common bile duct before passing through the pancreaticobiliary junction and entering the duodenum. After entering the PBJ, the pancreatic juice drains to the duodenum and does not go to the biliary part.

During the emptying phase, pancreaticobiliary reflux also was not found. Figure 4D-F shows the velocity magnitude, pressure distribution, and streamlines associated with this phase. In this stage, all fluids flow directly into the duodenum without changing expected directions.

The outcomes of our computational fluid dynamics simulations indicate that pancreaticobiliary reflux occurs during the gallbladder's refilling phase. Figure 5A-C illustrates the velocity magnitude, pressure distribution, and flow streamlines linked to this stage. Figure 5C demonstrates that pancreatic juice in PBJ bifurcates into two distinct streams. The first one flows towards the duodenum as expected. The other one flows to the common bile duct, subsequently reaching the gallbladder. The analysis suggests that a pressure differential between the gallbladder and duct system during the refilling phase is the principal driving force of PBR.

In the subsequent sections of this chapter, we investigate the factors influencing pancreaticobiliary reflux within our model (Table 1). To numerically quantify PBR, we determined the average flow rate across the half of the common bile duct (Q_{PBR}).This

Figure 4
Stationary and emptying phases

A. Stationary phase (velocity magnitude) **D.** Emptying phase (velocity magnitude)

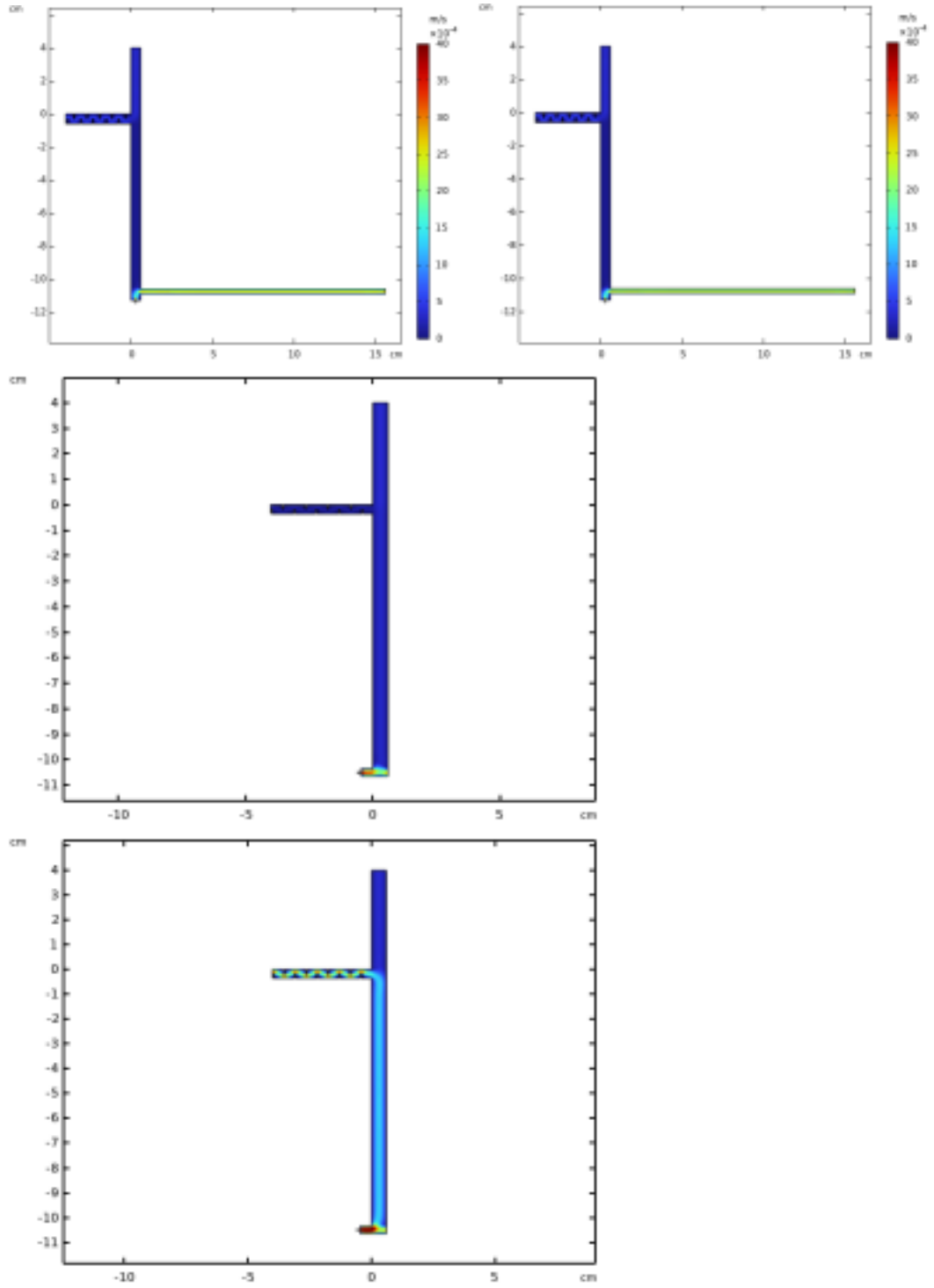

B. Stationary phase (pressure) **E.** Emptying phase (pressure)

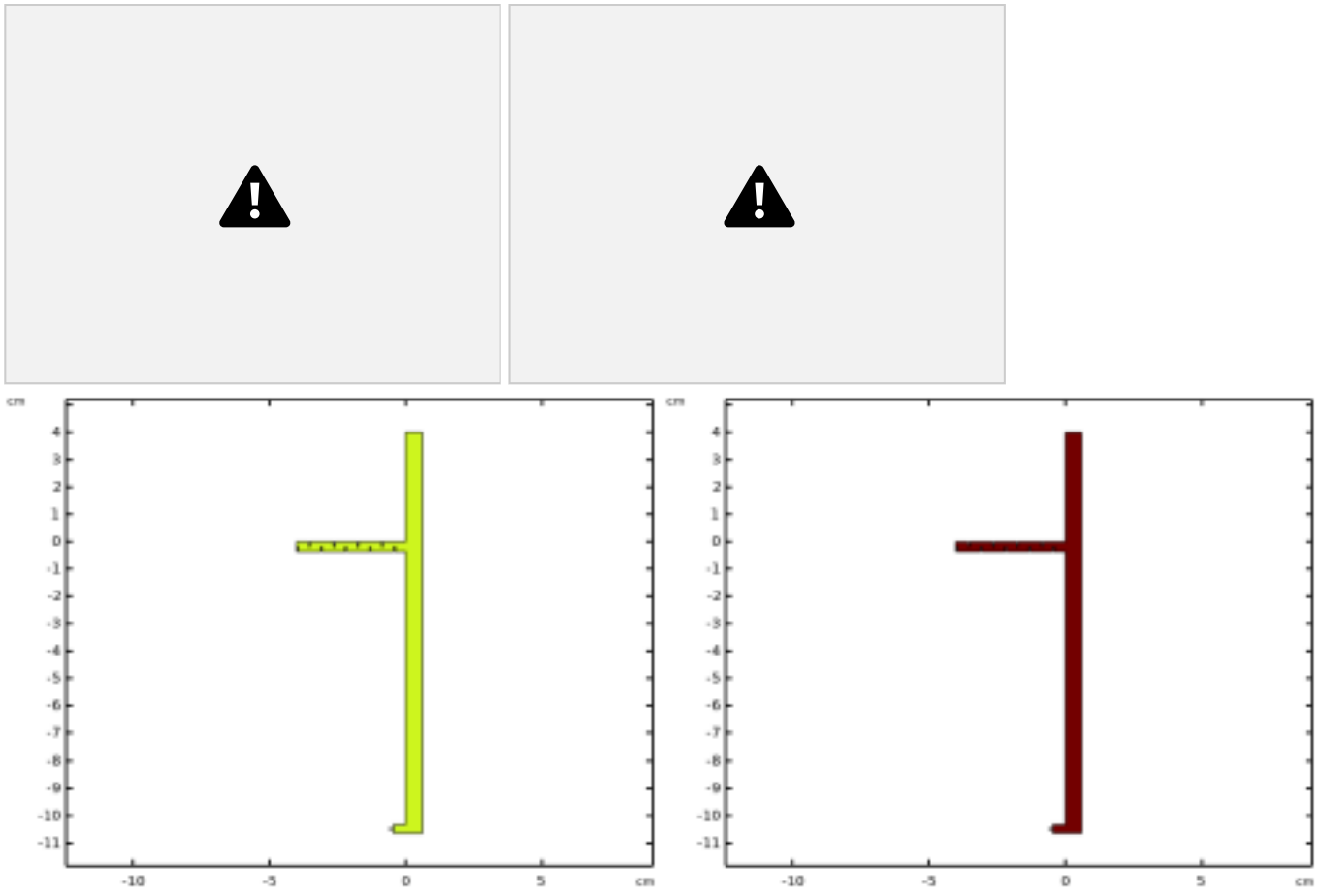

C. Stationary phase (streamlines from inlets) **F.** Emptying phase (streamlines from inlets)

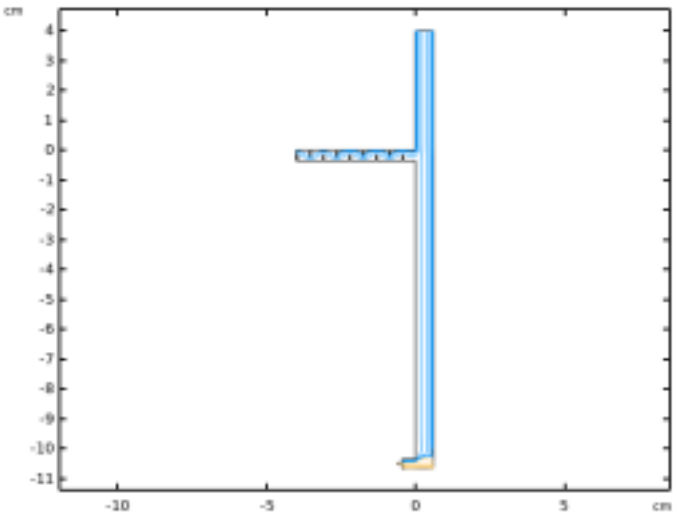

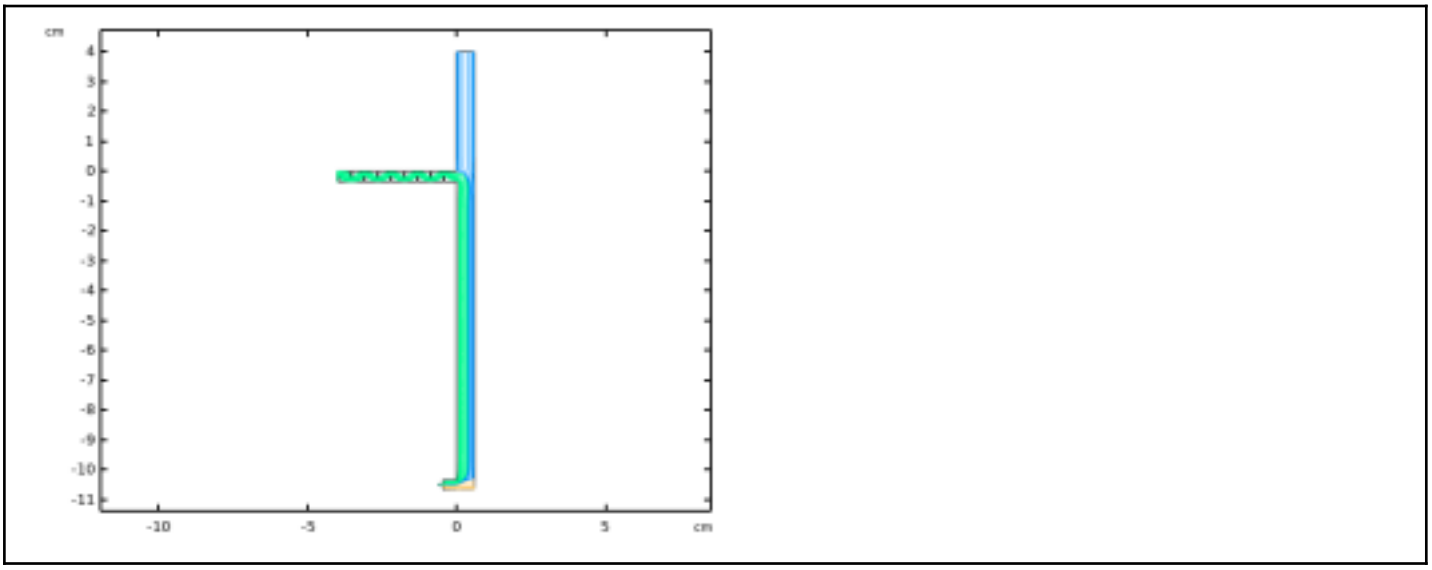

Figure 5

Refilling phase

A. Velocity magnitude **B.** Pressure

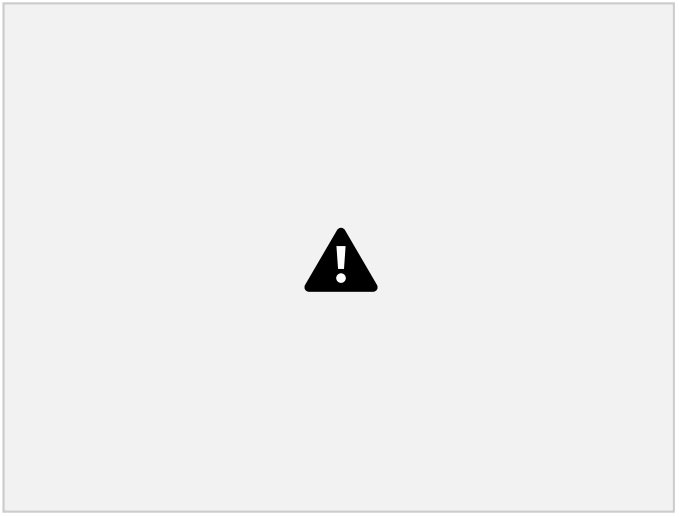

C. Streamlines from inlets

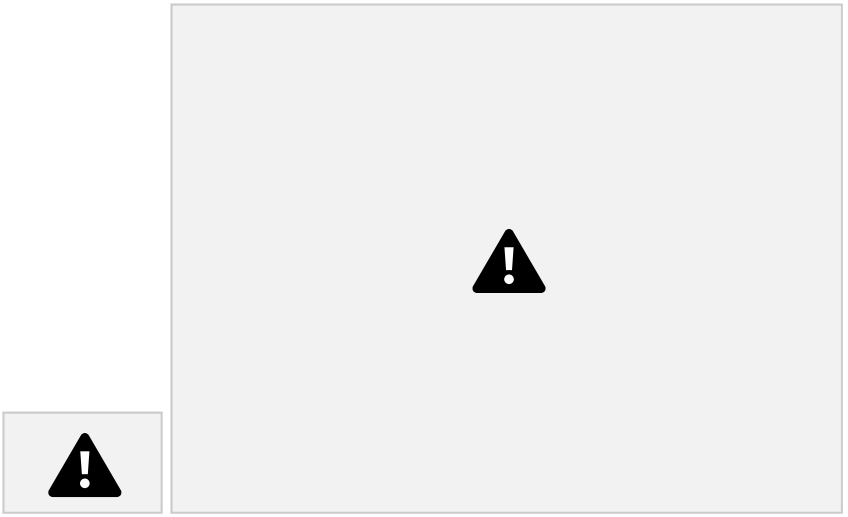

calculation was conducted utilising the equation $Q = A \times u$, where Q represents the flow rate, A is the cross-sectional area of the duct, and u denotes the velocity of the fluid flow. The cross-sectional area of the duct is derived from the formula $A = \pi \times \text{radius}^2$. For the common bile duct, this area was equal to $2.83 \times 10^{-5}\ m^2$.

3.2. Influence of pancreaticobiliary junction type

In this CFD simulation, different junction types (V, B-P, P-B) were created to evaluate the effect of junction type on PBR in pancreaticobiliary maljunction without biliary dilatation. The junction models were created according to Table 1, with visual representations in Figure 2 B-D.

The average flow rate in half of CBD in all types of junctions (V, B-P, P-B) during refilling phases was 1.40 ($\pm 4 \times 10^{-3}$) mL/min that suggests that the junction type does not

influence PBR.

3.3. Influence of common pancreaticobiliary duct channel length

This segment of the study explores how the length of the common pancreaticobiliary duct influences PBR in cases of pancreaticobiliary maljunction without biliary dilatation. To conduct this analysis, a parameter sweep for the CPBD length, ranging from 1 to 12 mm, was employed based on the model configurations listed in Table 1.

The findings from this investigation reveal that variations in the CPBD length do not significantly impact the occurrence of PBR. This conclusion is drawn from the observed data showing that Q_{PBR} remained consistent at 1.40 (± 6.66 × 10^{-4}) mL/min, regardless of the CPBD length adjustments. This stability in Q_{PBR} values across different CPBD lengths suggests that, within the parameters of our model, the length of the CPBD does not play a critical role in the development or prevention of PBR in the context of PBMWBD.

3.4. Influence of cystic duct diameter

The same approach as in the previous section was used to evaluate the effect of cystic duct diameter on PBR in PBMWBD. d_{CD} was set to its physiological range of 1-6 mm. The diameter of the cystic duct has a significant effect on PBR. Figure 6A illustrates the relationship between the cystic duct diameter and the average flow rate within half of the common bile duct (Q_{PBR}). Our observations reveal a minimum flow rate of 0.36 mL/min when the cystic duct diameter is 1 mm. Interestingly, as the diameter increases, Q_{PBR} escalates in a non-linear fashion up to a diameter of 4.5 mm. Beyond this point, we noted a consistent linear increase in Q_{PBR}, with a 0.01 mL/min increment for every 0.5 mm increase in diameter. Overall, the variation in cystic duct diameter resulted in an average Q_{PBR} of 1.23 (± 0.35) mL/min.

Further insights are provided in Figures 6B-D, which show the streamlines originating from the inlets in the T junction area near the cystic duct. When the diameter of the cystic duct is 1 mm, only two streamlines come to the gallbladder from the pancreatic segment of the pancreaticobiliary system. As the diameter increases, the flows from the pancreas also increase. For example, if d_{CD} is 6 mm, 7 of 10 streamlines originating from pancreas come to the gallbladder.

Figure 6
Influence of cystic duct diameter

A. B. $d_{CD} = 1$ mm

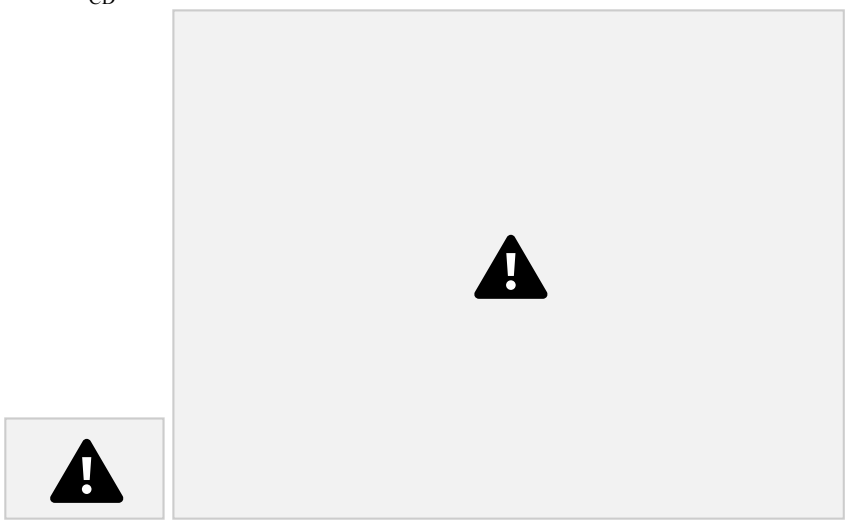

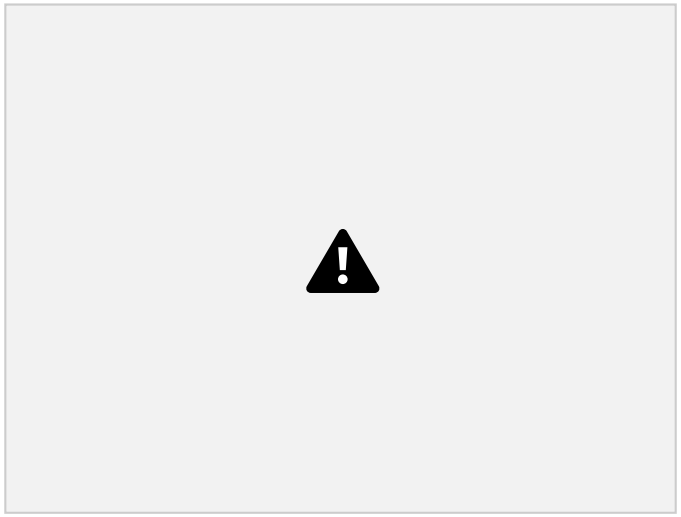

C. $d_{CD} = 3.5$ mm **D.** $d_{CD} = 6$ mm

3.5. Influences of number of baffles and baffle height ratio

In this section we investigated influence of the number of baffles (n_b) and the baffle height ratio ($_b\xi$) on PBR. For this purpose, the number of baffles was varied from 0 to 18, maintaining all other parameters as outlined in Table 1. Additionally, the baffle height ratio($_b$ ξ) was adjusted within the range of 0.2 to 0.7 to assess its effects. The results of these variations on Q_{PBR} are illustrated in Figures 7 and 8.

Figure 7A shows that the absence of baffles results in the highest observed Q_{PBR} (1.49 ml/min). The trend observed with increasing numbers of baffles is descending, however the rate of flow rate reduction is not constant. Initially, the flow rate decreases marginally with each additional baffle (-0.01 mL/min), subsequently undergoing periods of more rapid decline

Figure 7
Influence of number of baffles

A. B. n = 0

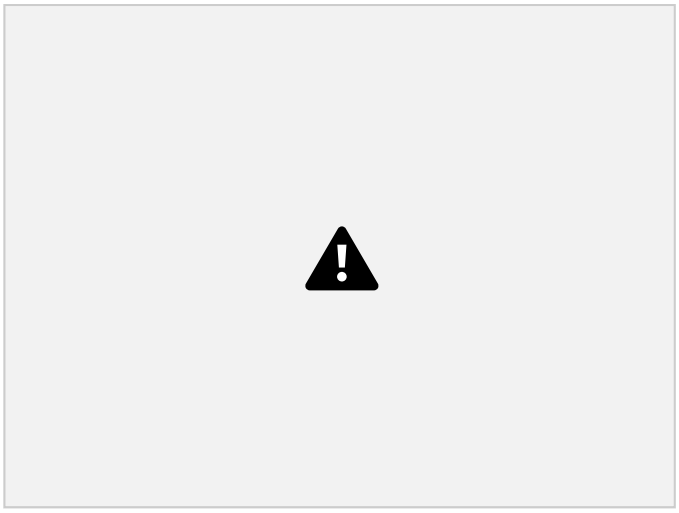

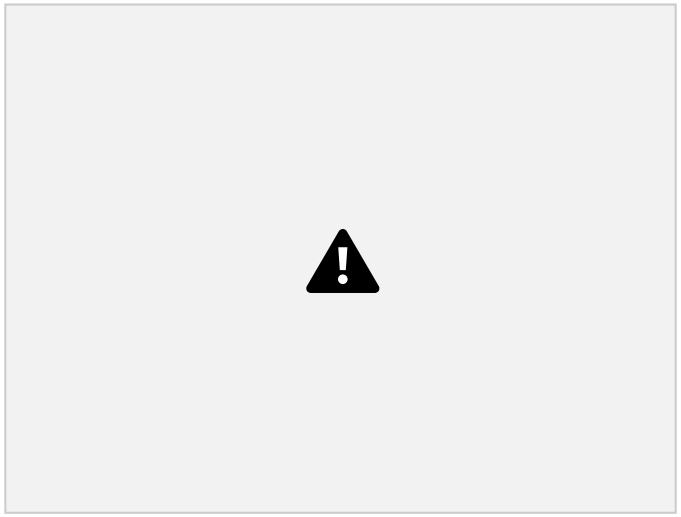

C. n = 9 **D.** n = 18

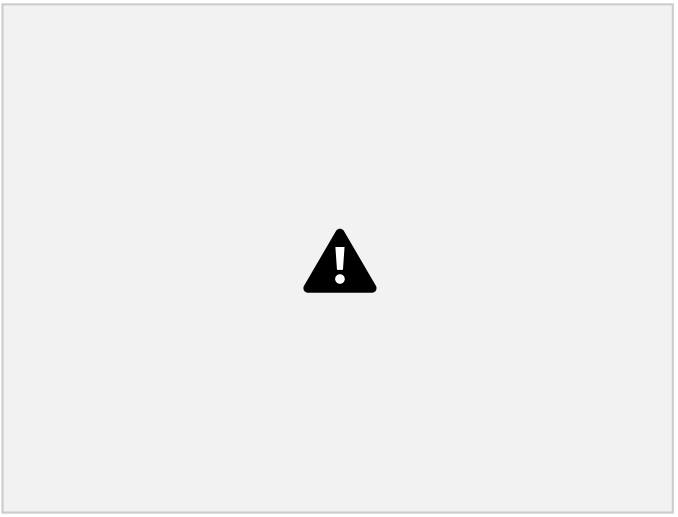

(-0.02 mL/min, -0.03 mL/min), including a phase of no change before accelerating the reduction rate towards the end (-0.05 mL/min per each additional baffle). This demonstrates that the number of baffles influences PBR, with an average Q_{PBR} recorded at 1.37 (± 0.1) mL/min during this parameter variation.

Figure 7B shows that 8 of 10 streamlines from the pancreatic duct reach the gallbladder in a system without baffles. However, if the system has 9 (Figure 7C) and 18 (Figure 7D) baffles, 6 of 10 and 4 of 10 streamlines, respectively, come to the gallbladder from the pancreas.

Figure 8A shows the variation in Q_{PBR} as the baffle height ratio changes, highlighting a non-linear descending trend. The rate of change in Q_{PBR} accelerates with an increase in the

baffle height ratio. Across these variations, the average Q_{PBR} was found to be 1.38 (± 0.12) mL/min.

Figures 8B-D show change in streamlines coming from the pancreas with varying baffle height ratios. Specifically, for baffle height ratios of 0.2, 0.5, and 0.7, the proportions of streamlines reaching the gallbladder are 7/10, 6/10, and 4/10, respectively.

These findings underscore the role of baffle configuration (n_b and $_b\xi$) in modulating PBR.

Figure 8
Influence of baffle height ratio

A. B. $\xi_b = 0.2$

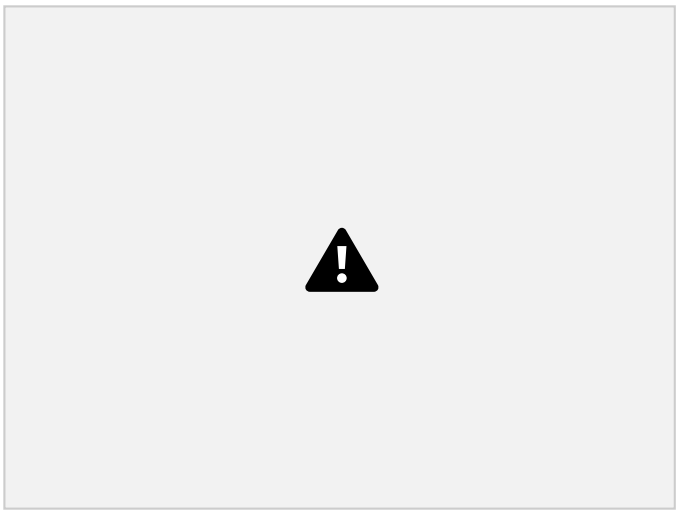

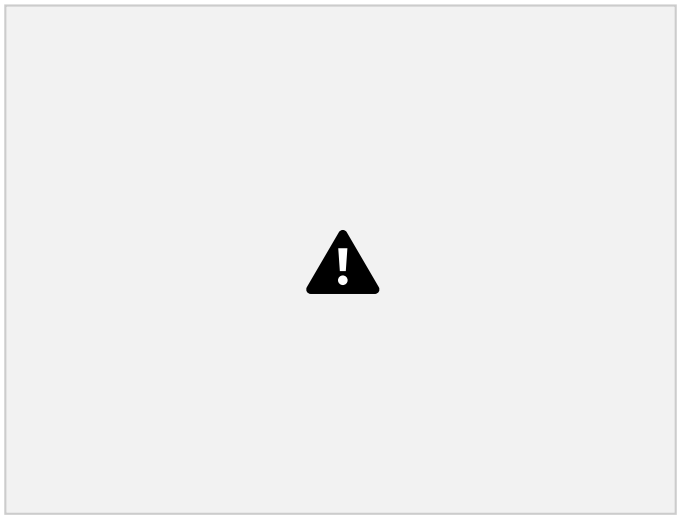

C. $_b = 0.5$ **D.** $\xi\ \xi_b = 0.7$

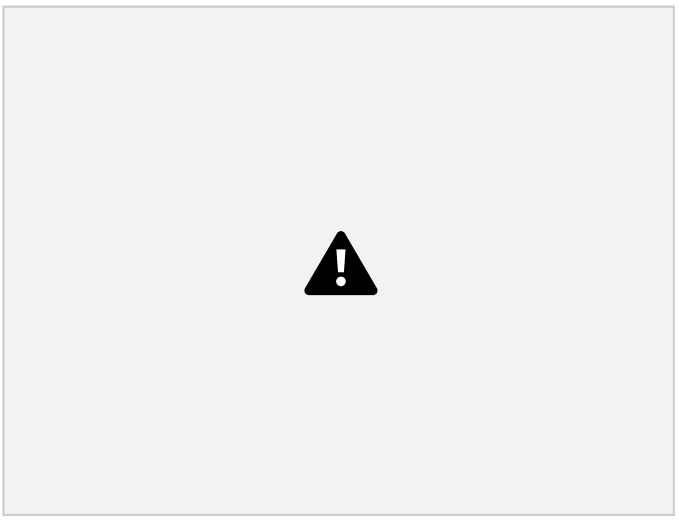

3.6. Influences of fluid viscosity and rheological behaviour

Several studies have developed non-Newtonian models of bile juice. Carreau and Casson-Papanastasiou models of bile are shown in Appendix Tables 2 and 3. Li et al. (2008) developed the Carreau model of bile based on Gottschalk and Lochner (1990) and Coene et al. (1994) studies. Because duct bile is used in these studies, this model is suitable for representing duct bile. The Casson model developed by Saida (1992) represents gallbladder bile. Kuchumov et al. (2014) developed a Carreau and Casson model for pathological bile.

Figure 9 shows a dataset on the dynamic viscosity of bile from various studies alongside non-Newtonian models proposed by Li et al. (2008) and Saida (1992). This figure illustrates that the viscosity of gallbladder bile is significantly higher than that of bile from the duct. Moreover, the models developed by Li et al.(2008) and Saida (1992) demonstrate a concordance with data from other studies.

Figure 9
Dynamic viscosity of bile juice

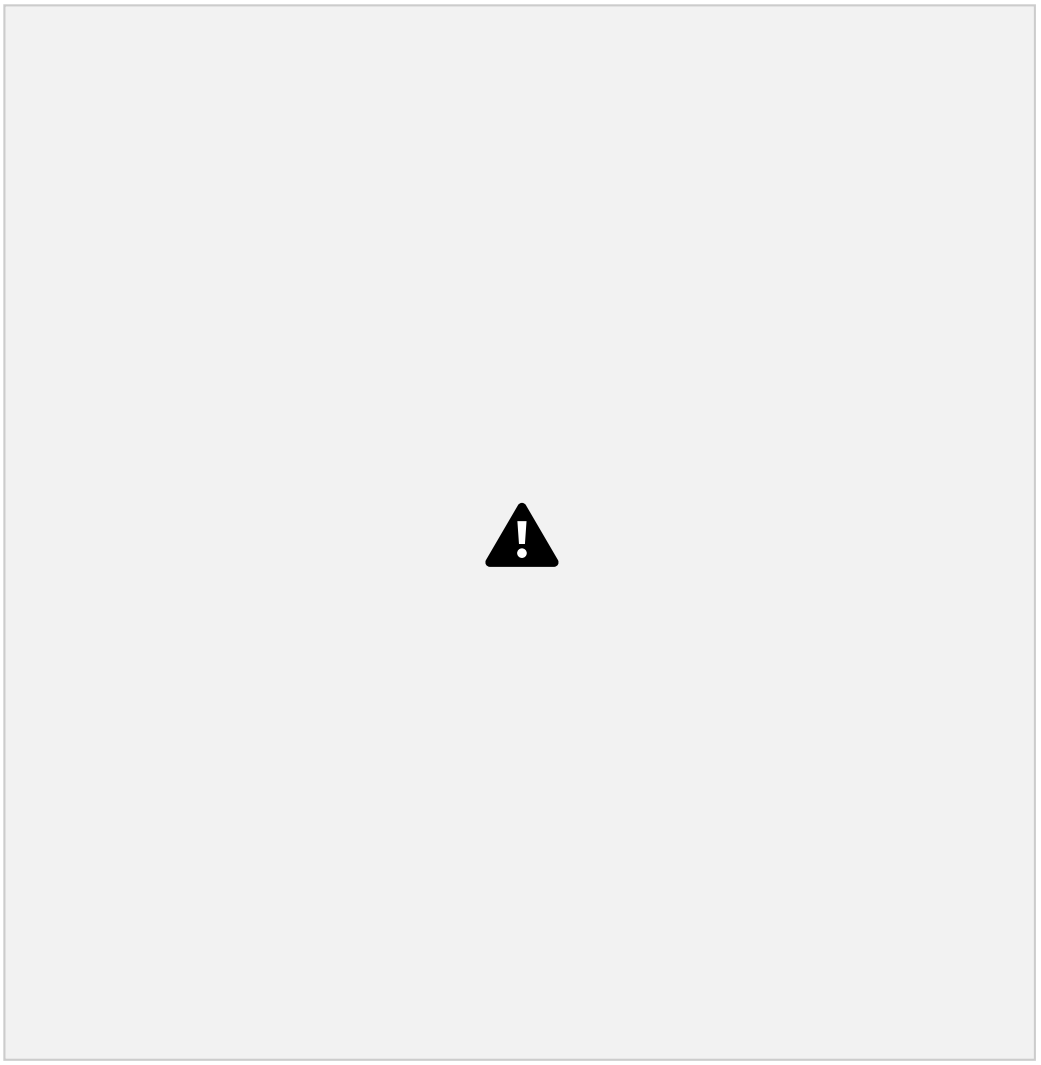

In this CFD study, we investigate the effect of fluid viscosity on PBR in PBMWBD during the refilling phase using our one-fluid model. The experiment used the fluid's dynamic viscosity within a range of 1 to 10 mPa·s, encapsulating most viscosity ranges observed in pancreaticobiliary system fluids (see Appendix Table 1). Non-Newtonian models from Li et al. (2008) and Saida (1992) were also applied in this study. In the Casson-Papanastasiou equation we used m = 10.

The findings from our results indicate that variations in fluid viscosity and rheological behaviour has minimal influence on pancreaticobiliary reflux within our computational model. Throughout the range of viscosity modifications (1-10 mPa × s), the average Q_{PBR} remained consistent at 1.40 ($\pm$ 2.32 × 10^{-3}) mL/min. A comparative assessment of non-Newtonian versus Newtonian fluid models revealed a little difference in Q_{PBR}, with non-Newtonian models registering a slightly lower flow rate (1.39 mL/min) compared to Newtonian model (1.40 mL/min). The reason that Q_{PBR} in non-Newtonian models is quite the same as Q_{PBR} in Newtonian models is because shear rate in the PBS where reflux is observed is low. These

observations underscore that rheological properties in one-fluid model do not significantly impact PBR.

3.7. Discussion

The simulation showed that pancreaticobiliary reflux occurs in PBMWBD during the refilling phase, corroborating the conclusions drawn by Tajikawa et al. (2023) and Fukuzawa et al. (2020).

Fukuzawa et al. (2020) highlighted a scenario where reflux could manifest even during the stationary phase if the gallbladder's absorption rate (Q_{GBa}) exceeds the liver's bile production rate (Q_{CHD}). The authors used Q_{GBa} equal to 46 mL/h in their study to explore this phenomenon. The possible reason for such reflux in their experimental setup is that absorption was mechanically modulated directly from the cystic duct, diverging from physiological processes where absorption primarily occurs through the gallbladder wall.

In our investigation, we used the simulation of absorption by implementing a fully developed flow outlet, with the exit's thickness mirroring the width of the gallbladder, to approximate the absorption dynamics. Under these conditions, our model did not exhibit reflux, even when Q_{GBa} was increased to 46 mL/h. It is crucial to acknowledge that our absorption modelling still deviates significantly from the complex physiological process of absorption in the gallbladder.

Our results suggest that the type of PBJ does not significantly influence PBR. This conclusion is drawn from our simulations, which shows consistent PBR metrics across various junction types.

The findings from our study indicate that the length of the common pancreaticobiliary duct has no significant impact on pancreaticobiliary reflux. Kamisawa et al. (2002) stated that a long common pancreaticobiliary duct in normal cases when PBJ occurs under the region of sphincter Oddi influences PBR. However, according to our data, within the context of pancreaticobiliary maljunction, these anatomical features do not impact PBR.

Li et al. (2007) identified the diameter of the cystic duct as the paramount factor influencing the pressure drop during the gallbladder's emptying phase. Furthermore, they noted that the baffle height ratio and the number of baffles also play a role in modulating the pressure drop throughout the emptying phase. Building on this foundation, Tajikawa et al. (2023) proposed that the specific configuration of the cystic duct serves as a protective mechanism against pancreaticobiliary reflux during the refilling phase. Our research findings

support this hypothesis.

While our data indicate that fluid properties do not significantly impact PBR, it's important to consider that our model does not fully simulate the pancreaticobiliary system, which essentially operates as a three-fluid system.

In our study, we did not explore the effect of variations in the length of the cystic duct (L_{CD}) or in the specific anatomical location where the common bile duct, common hepatic duct, and cystic duct connected on PBR. However, both of these parameters could influence pancreaticobiliary reflux. Future research could benefit from a detailed examination of these features.

The study findings highlight the importance of the gallbladder's phases in the development of PBR and suggest potential areas for further research and clinical investigation. Understanding these mechanisms is essential for the development of more effective diagnostic and therapeutic strategies for managing disorders associated with PBR.

Chapter 4 – Effect of surgical procedures on pancreatic juice reflux in pancreaticobiliary maljunction without biliary dilatation

4.1. Cholecystectomy

This CFD study investigated the pancreaticobiliary system in patients with PBMWBD who have undergone a cholecystectomy (removal of the gallbladder). During a cholecystectomy, surgeons try to remove the cystic duct as much as possible because cystic duct remnants longer than 10 mm can cause the persistence of biliary colic after removal, which is called postcholecystectomy syndrome (Bodvall & Overgaard, 1965). Therefore, in our model the L_{CD} was set to 10 mm, n_b was set to 0. Due to the gallbladder's removal, its phases no longer influence PBS fluid dynamics. Therefore, our model has two inlets representing liver (Q_{CHD}) and pancreatic (Q_{PD}) secretions and one outlet into the duodenum (P_{duo}).

Figure 10 illustrates the distribution of velocity magnitude, pressure, and streamlines in PBS after cholecystectomy. The visual data clearly demonstrate that after the removal of the gallbladder, pancreaticobiliary reflux does not occur.

4.2. Endoscopic retrograde cholangiopancreatography

In this computational fluid dynamics simulation, papillary balloon dilation procedure by the Endoscopic Retrograde Cholangiopancreatography (ERCP) was modelled . To simulate this procedure, the $d_{CPBD\text{-}RSO}$ was adjusted within a range of 0.3 to 6 mm. Additionally, we investigated variations in the diameter of the cystic duct (d_{CD}) on efficiency of this procedure. Because PBR occurs during the refilling phase, our simulations were specifically focused on this phase.

ERCP's papillary balloon dilation shows potential in treating PBR in PBMWBD. Figure 11 illustrates how papillary balloon dilation influences Q_{PBR} by modifying the diameter of the common pancreaticobiliary duct in the region of the sphincter of Oddi. Initially, as shown in Figure 11A, increasing the diameter of the common pancreaticobiliary duct in the sphincter Oddi region leads to a decrease and then an increase in the average flow rate within the common bile duct. This dynamic is clarified in Figures 11B-D.

Figure 10
Post-cholecystectomy

A. Velocity magnitude **B.** Pressure

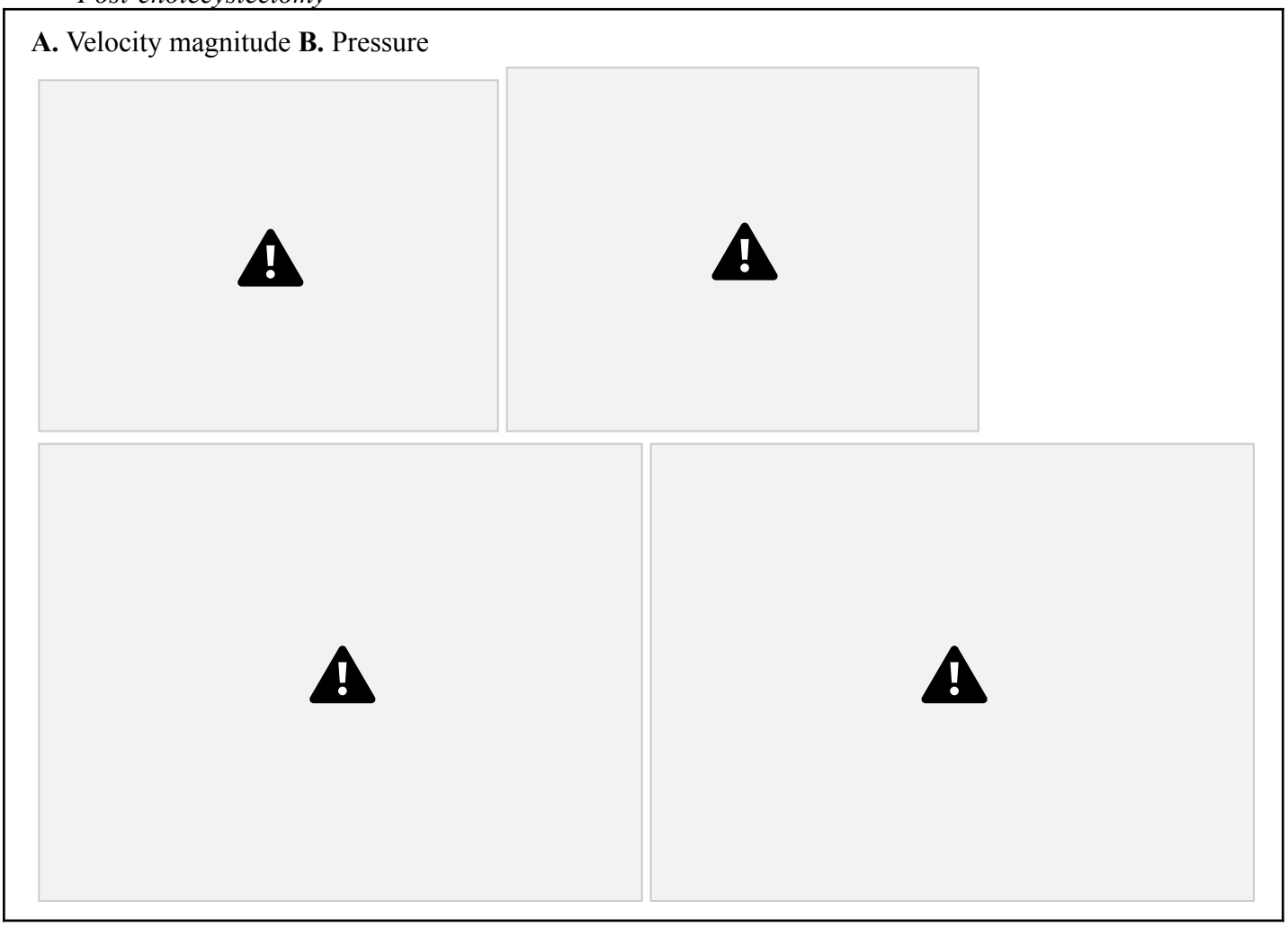

C. Streamlines from inlets

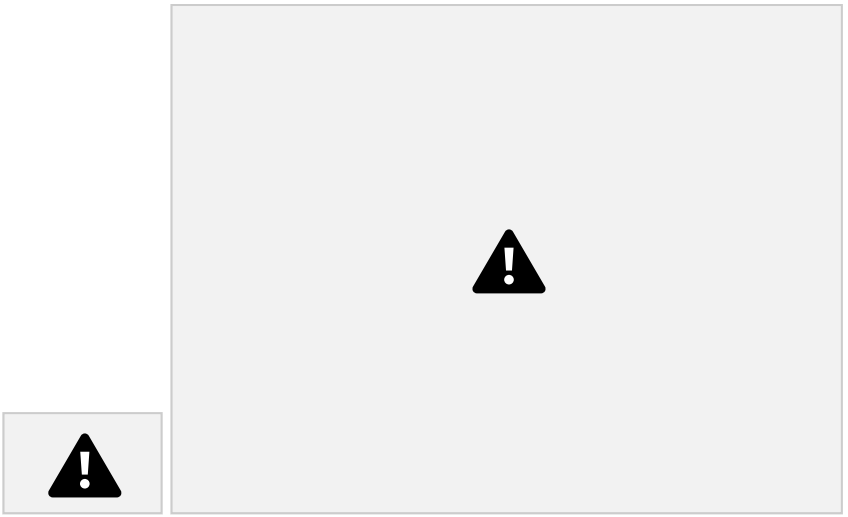

Figure 11B shows PBR when the $d_{CPBD\text{-}RSO}$ is 0.3 mm. In contrast, Figure 11C demonstrates the absence of reflux when the $d_{CPBD\text{-}RSO}$ is expanded to 1.3 mm, indicating an optimal diameter for preventing PBR. When the $d_{CPBD\text{-}RSO}$ is increased to 1.5 mm, bile from the liver flows towards the duodenum, as shown in Figure 11D.

Figure 12 demonstrates the relationship between d_{CD} and $d_{CPBD\text{-}RSO}$ at which minimal Q_{PBR} is observed. The data suggests that to prevent PBR, papillary balloon dilatation should increase the diameter of CPBD-RSO to at least 45% of the diameter of the cystic duct.

Figure 11
ERCP effect on PBR

A. B. $d_{CPBD\text{-}RSO}$ = 0.3 mm, d_{CD} = 3.5 mm

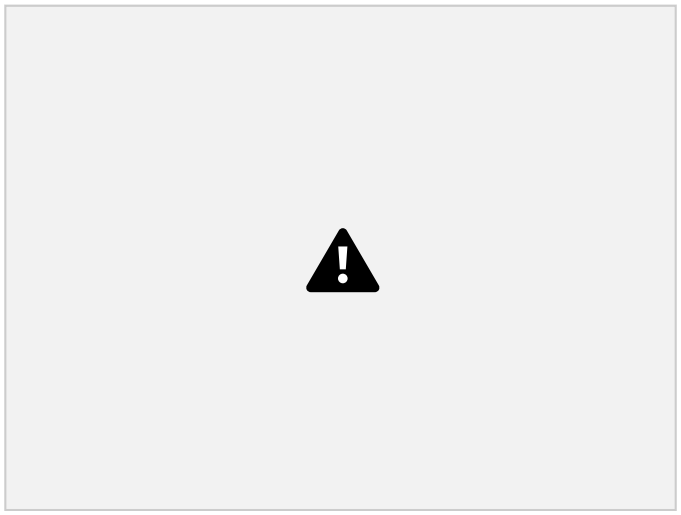

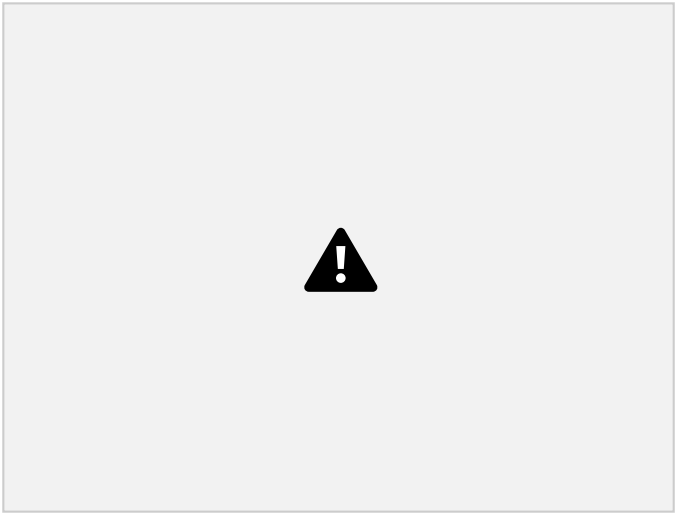

C. $d_{CPBD\text{-}RSO} = 1.3$ mm, $d_{CD} = 3.5$ mm **D.** $d_{CPBD\text{-}RSO} = 1.5$ mm, $d_{CD} = 3.5$ mm

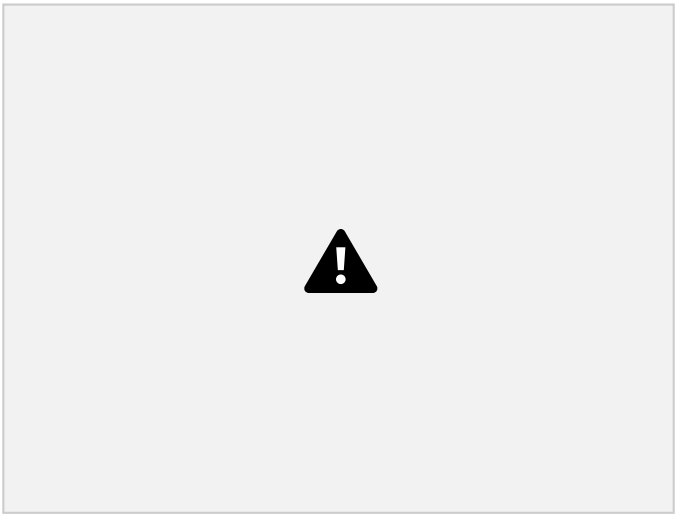

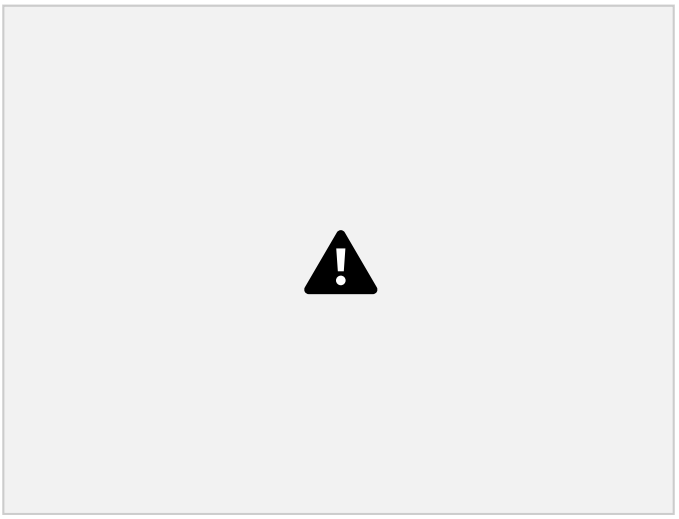

4.3. Discussion

According to Kamisawa et al. (2012), individuals with PBM should consider surgery to

reduce the risk factor for biliary cancer, even if they do not have symptoms. However, in the context of PBMWBD, no standard surgical treatment currently exists (Qian et al., 2023). Irrespective of the presence or absence of biliary dilatation, hepaticoenterostomy combined with removal of the extrahepatic bile duct, is one of the most common surgical interventions for PBM (Urushihara et al., 2017). A comparative analysis of the outcomes of ERCP and laparoscopic hepaticojejunostomy (type of hepaticoenterostomy) conducted by Qian et al. (2023) revealed that hepaticojejunostomy tends to be more effective than ERCP in treating

Figure 12

Correlation between d_{CD} and $d_{CPBD\text{-}RSO}$ at which minimal Q_{PBR} is observed

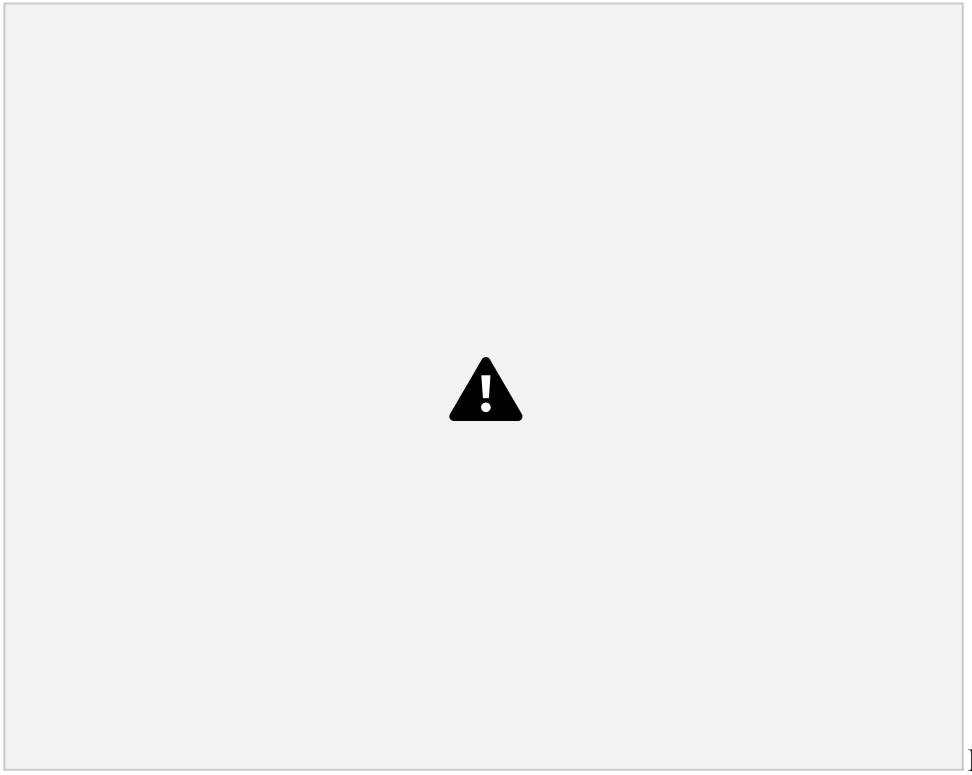

PBMWBD.

However, it is also associated with longer operation time and postoperative recovery time and has more incidence of postoperative complications compared to ERCP. Our results provided a quantifiable target for optimising ERCP interventions that can potentially improve ERCP efficiency.

Recent studies by Fukuzawa et al. (2020) and Tajikawa et al. (2023) have proposed that cholecystectomy could serve as an effective intervention to treat PBR in cases of PBMWBD. However, this operation is not universally accepted as a treatment option for PBMWBD (Qian et al., 2023). Our CFD simulation supports the efficacy of cholecystectomy as a potential treatment strategy for managing PBR in PBMWBD,

While our study provides insights into the impact of ERCP and cholecystectomy on

pancreaticobiliary reflux in cases of pancreaticobiliary maljunction without biliary dilatation, validating these findings through clinical or animal studies is essential. Such empirical research is necessary to confirm or refute our simulated outcomes, offering a more reliable understanding of these interventions' effectiveness.

The use of computational fluid dynamics offers a promising avenue for personalised medicine, particularly in predicting the outcomes of surgical interventions. Our model has the potential for customization based on patient-specific individual geometry, which can be

accurately captured through imaging techniques like magnetic resonance cholangiopancreatography or ultrasound.

Chapter 5 - Conclusion

5.1. Summary of findings

Study data suggests that the primary mechanism for pancreaticobiliary reflux in pancreaticobiliary maljunction without biliary dilatation is the refilling phase. No reflux was observed during the emptying and stationary phases.

The diameter of the cystic duct emerges as the most crucial determinant of pancreaticobiliary reflux. Furthermore, the configuration of the baffle system, including its height ratio and the number of baffles, also plays a significant role in modulating pancreaticobiliary reflux dynamics.

Our research findings suggest that the type of pancreaticobiliary junction and the length of the common pancreaticobiliary duct do not significantly impact pancreaticobiliary reflux. Moreover, our one-fluid model indicates that the rheological properties of fluids have little influence on pancreaticobiliary reflux.

Cholecystectomy can be a potential therapeutic avenue for addressing pancreaticobiliary reflux in pancreaticobiliary maljunction without biliary dilatation. Additionally, interventions such as balloon dilation by endoscopic retrograde cholangiopancreatography hold promise in mitigating pancreaticobiliary reflux in pancreaticobiliary maljunction without biliary dilatation, when the diameter of the common pancreaticobiliary duct will be dilated to approximately 45% that of the cystic duct.

5.2. Summary of limitations

The work has several limitations. Firstly, the developed model does not account for the phasic contraction of the sphincter of Oddi. Secondly, the stationary solver used in the model may not be ideal for the emptying phase. Using a time-dependent solver is more suitable during this phase. Thirdly, hepatic and pancreatic flow rates are based on assumptions from previously published studies rather than individual patient data. Fourthly, our model of gallbladder absorption only partially encompasses the complex physiological process involved. Lastly, the model operates under the assumption of a single fluid in the pancreaticobiliary system, while in reality, it is a three-fluid system. By solving these limitations, researchers can improve the model.

5.3. Future research

Based on our work, several computational fluid dynamics studies can be conducted. The model we have developed has the potential to be reconfigured to simulate the anatomically normal junction and HCPBD. To achieve this, Oddi's sphincter region must include the entire CPBD and some parts of CBD and PD. Through this reconfiguration, we could study the features that influence reflexes in these anatomical configurations.

In addition to this, the model can also be reconfigured to study PBR and the impact of surgeries on other types of PBM (such as stenotic, dilated, and complex types). To achieve this, fluid-structure interaction could be implemented in future models.

Furthermore, the developed model could be modified to study biliopancreatic reflux in the pancreaticobiliary system. For this, the head part of the major pancreatic duct should be added to the model, and hepatic and pancreatic flow rate variations should be applied.

Moreover, variations in the length of the cystic duct or variations in the location of the cystic duct junction could be studied to estimate the impact of these anatomical features on refluxes in the developed model.

Lastly, possible future research could include evaluating our 2D idealised model with a 3D idealised model and patient-specific 3D model of PBS obtained from magnetic resonance cholangiopancreatography scans.

The study results provide a justified direction for further clinical and animal research to improve the treatment of patients with pancreaticobiliary maljunction without biliary dilatation and understand the mechanism of pancreaticobiliary reflux.

One possible clinical trial could be a randomised prospective study that separates patients with PBMWBD into three treatment groups to evaluate efficiency (absence of

PBMWBD symptoms after operation) and safety (postoperative complications). The first group will be treated by cholecystectomy, the second group with ERCP intervention that will increase the diameter of CPBD to 45% of the diameter of CD, and the last group will serve as a control group and be treated with hepaticoenterostomy. This possible research could validate or reject the results of our study.

References

Al-Atabi, M., Ooi, R., Luo, X., Chin, S. B., & Bird, N. C. (2012). Computational analysis of the flow of bile in human cystic duct. *Medical Engineering & Physics, 34*(8), 1177–1183. https://doi.org/10.1016/j.medengphy.2011.12.006

Arnolds. (1906). Eine manneskopfgroßen retentionszyste des choledochus. *Deutsche Medizinische Wochenschrift*, *32*(44).

Baghaei, M., Kavian, M., Ghodsi, S., & Razavi, S. E. (2021). Numerical investigation of bile secretion and pressure rise in obstructed human common bile duct. *Journal of Applied Fluid Mechanics., 14*(01). https://doi.org/10.47176/jafm.14.01.31309

Bodvall, B., & Overgaard, B. (1966). Cystic duct remnant after cholecystectomy. *Annals of Surgery*, *163*(3), 382–390. https://doi.org/10.1097/00000658-196603000-00009 Bouchier, I. a. D., Cooperband, S. R., & Kodsi, B. M. E. (1965). Mucous substances and viscosity of normal and pathological human bile. *Gastroenterology*, *49*(4), 343–353. https://doi.org/10.1016/s0016-5085(19)34508-1

Boyer, J. L. (2013). Bile formation and secretion. *Comprehensive Physiology*, 1035–1078. https://doi.org/10.1002/cphy.c120027

Coene, P. P. L. O., Groen, A. K., Davids, P. H. P., Hardeman, M. R., Tytgat, G. N. J., & Huibregtse, K. (1994). Bile Viscosity in Patients with Biliary Drainage: Effect of Co-Trimoxazole andN-Acetylcysteine and Role in Stent Clogging. *Scandinavian Journal of Gastroenterology*, *29*(8), 757–763. https://doi.org/10.3109/00365529409092506

Cowie, A. G. A., & Sutor, D. J. (1975). Viscosity and osmolality of abnormal biles. *Digestion*, *13*(5), 312–315. https://doi.org/10.1159/000197724

Da, X., Xiang, Y., Hu, H., Kong, X., Qiu, C., Jiang, Z., Zhao, G., Cai, J., Huang, A., Zhang, C., He, C., Lv, B., Zhang, H., & Yang, Y. (2024). Identification of changes in bile composition in pancreaticobiliary reflux based on liquid chromatography/mass spectrometry metabolomics. *BMC Gastroenterology*, *24*(1). https://doi.org/10.1186/s12876-023-03097-4

Fukuzawa, H., Kajihara, K., Tajikawa, T., Aoki, K., Ajiki, T., & Murakami, K. (2020). Mechanism of pancreatic juice reflux in pancreaticobiliary maljunction: A fluid dynamics model experiment. *Journal of Hepato-Biliary-Pancreatic Sciences*, *27*(5), 265–272. https://doi.org/10.1002/jhbp.714

Gründel, D., Jüngst, C., Straub, G., Althaus, R., Schneider, B., Spelsberg, F., Hüttl, T. P., Del Pozo, R., Jüngst, D., & Neubrand, M. (2009). Relation of Gallbladder Motility to Viscosity and Composition of Gallbladder Bile in Patients with Cholesterol Gallstones. *Digestion*, *79*(4), 229–234. https://doi.org/10.1159/000213828

Harada, H., Ueda, O., Kochi, F., Kobayashi, T., & Komazawa, M. (1981). Comparative studies on viscosity and concentration of protein and hexosamine in pure pancreatic

juice. *Gastroenterologia Japonica*, *16*(6), 623–626. https://doi.org/10.1007/bf02813799

Housset, C., Chrétien, Y., Debray, D., & Chignard, N. (2016). Functions of the gallbladder. *Comprehensive Physiology*, 1549–1577. https://doi.org/10.1002/cphy.c150050 Howard, P. J., Murphy, G., & Dowling, R. H. (1991). Gall bladder emptying patterns in response to a normal meal in healthy subjects and patients with gallstones: ultrasound study. *Gut*, *32*(11), 1406–1411. https://doi.org/10.1136/gut.32.11.1406

Jüngst, D., Niemeyer, A., Müller, I., Zündt, B., Meyer, G., Wilhelmi, M., & Del Pozo, R. (2001). Mucin and phospholipids determine viscosity of gallbladder bile in patients

with gallstones. *World Journal of Gastroenterology*, *7*(2), 203. https://doi.org/10.3748/wjg.v7.i2.203

Kamisawa, T., Amemiya, K., Tu, Y., Egawa, N., Sakaki, N., Tsuruta, K., Okamoto, A., & Munakata, A. (2002). Clinical significance of a long common channel. *Pancreatology*, *2*(2), 122–128. https://doi.org/10.1159/000055902

Kamisawa, T., Ando, H., Suyama, M., Shimada, M., Morine, Y., & Shimada, H. (2012). Japanese clinical practice guidelines for pancreaticobiliary maljunction. *Journal of Gastroenterology*, *47*(7), 731–759. https://doi.org/10.1007/s00535-012-0611-2

Kaneko, K., Ando, H., Seo, T., Ono, Y., Tainaka, T., & Sumida, W. (2007). Proteomic Analysis of Protein Plugs: Causative Agent of Symptoms in Patients with Choledochal Cyst. *Digestive Diseases and Sciences*, *52*(8), 1979–1986. https://doi.org/10.1007/s10620-006-9398-4

Kim, E. Y., & Hong, T. H. (2020). Bile cholesterol and viscosity, the keys to discriminating adenomatous polyps from cholesterol polyps by a novel predictive scoring model. *BMC Gastroenterology*, *20*(1). https://doi.org/10.1186/s12876-020-01414-9

Kuchumov, A. G. (2019). Patient-Specific bile flow simulation to evaluate cholecystectomy outcome. *IOP Conference Series: Materials Science and Engineering,* 581(1), 012022. https://doi.org/10.1088/1757-899x/581/1/012022

Kuchumov, A. G., Kamaltdinov, Samarcev, V. A., Khairulin, A. R., Ivashova, Y. A., & Taiar, R. (2020). Patient-specific simulation of a gallbladder refilling based on MRI and ultrasound in vivo measurements. *AIP Conference Proceedings.* https://doi.org/10.1063/5.0003367

Kuchumov, A. G., Gilev, V. G., Popov, V. V., Samarcev, V. A., & Gavrilov, V. A. (2014). Non-Newtonian flow of pathological bile in the biliary system: experimental investigation and CFD simulations. *Korea-australia Rheology Journal*, *26*(1), 81–90. https://doi.org/10.1007/s13367-014-0009-1

Kuchumov, A. G., Tuktamyshev, V., & Kamaltdinov. (2017). Peristaltic flow of lithogenic bile in the vateri's papilla as non-newtonian fluid in the finite-length tube: Analytical and numerical results for reflux study and optimization. *Lékař a Technika - Clinician and Technology, 4*7(2), 35–42.

Li, W. (2021). *Biliary Tract and Gallbladder Biomechanical Modelling with Physiological and Clinical Elements*. CRC Press.

Li, W. G., Luo, X., Johnson, A. G., Hill, N. M., Bird, N. C., & Chin, S. B. (2007). One-Dimensional models of the human biliary system. *Journal of Biomechanical Engineering*, *129*(2), 164–173. https://doi.org/10.1115/1.2472379

Li, W., Luo, X., Chin, S. B., Hill, N. M., Ag, J., & Bird, N. C. (2008). Non-Newtonian bile flow in elastic cystic duct: One- and Three-Dimensional modeling. *Annals of Biomedical Engineering*, *36*(11), 1893–1908. https://doi.org/10.1007/s10439

-008-9563-3
Meyer, K., Ostrenko, O., Bourantas, G. C., Morales‐Navarrete, H., Porat-Shliom, N., Segovia-Miranda, F., Nonaka, H., Ghaemi, A., Verbavatz, J., Brusch, L., Sbalzarini, I. F., Kalaidzidis, Y., Weigert, R., & Zerial, M. (2017). A predictive 3D Multi-Scale model of biliary fluid dynamics in the liver lobule. *Cell Systems, 4*(3), 277-290. https://doi.org/10.1016/j.cels.2017.02.008
Misra, S. P., & Dwivedi, M. (1990). Pancreaticobiliary ductal union. *Gut*, *31*(10), 1144–1149. https://doi.org/10.1136/gut.31.10.1144
Möller, K., Jenssen, C., Ignee, A., Hocke, M., Faiss, S., Iglesias‐García, J., Sun, S., Dong, Y., & Dietrich, C. (2023). Pancreatic duct imaging during aging. *Endoscopic Ultrasound*, *12*(2), 200. https://doi.org/10.4103/eus-d-22-00119

Morine, Y., Shimada, M., Takamatsu, H., Araida, T., Endo, I., Kubota, M., Toki, A., Noda, T., Matsumura, T., Miyakawa, S., Ishibashi, H., Kamisawa, T., & Shimada, H. (2013). Clinical features of pancreaticobiliary maljunction: update analysis of 2nd Japan‐nationwide survey. *Journal of Hepato-biliary-pancreatic Sciences (Print)*, *20*(5), 472–480. https://doi.org/10.1007/s00534-013-0606-2
Muraki, T., Reid, M. D., Pehlivanoğlu, B., González, R., Sekhar, A., Memiş, B., Xue, Y., Cheng, J., Jang, K. T., Mittal, P., Cardona, K., Kooby, D. A., Maithel, S. K., Sarmiento, J. M., El‐Rayes, B. F., Lomberk, G., Urrutia, R., Christians, K. K., Tsai, S., . . . Adsay, V. (2020). Variant anatomy of the biliary system as a cause of pancreatic and peri-ampullary cancers. *HPB*, *22*(12), 1675–1685. https://doi.org/10.1016/j.hpb.2020.03.014
Nylund, K., Hausken, T., Ødegaard, S., Eide, G. E., & Gilja, O. H. (2012). Gastrointestinal Wall Thickness Measured with Transabdominal Ultrasonography and Its Relationship to Demographic Factors in Healthy Subjects. *European Journal of Ultrasound - Ultraschall in Der Medizin*, *33*(07), E225–E232. https://doi.org/10.1055/s-0031-1299329
Okazaki, K., Yamamoto, Y., & Ito, K. (1986). Endoscopic measurement of papillary sphincter zone and pancreatic main ductal pressure in patients with chronic pancreatitis. *Gastroenterology*, *91*(2), 409–418. https://doi.org/10.1016/0016-5085(86)90576-7
Ono, A., Arizono, S., Isoda, H., & Togashi, K. (2020). Imaging of pancreaticobiliary maljunction. *Radiographics*, *40*(2), 378–392. https://doi.org/10.1148/rg.2020190108 Ooi, R., Luo, X., Chin, S. B., Johnson, A. G., & Bird, N. C. (2004). The flow of bile in the human cystic duct. *Journal of Biomechanics*, *37*(12), 1913–1922. https://doi.org/10.1016/j.jbiomech.2004.02.029
Ooi, R. C., Luo, X. Y., Chin, S. B., Johnson, A. G., & Bird, N. (2003, June). Fluid-structure interaction (FSI) simulation of the human cystic duct. In *Summer bioengineering conference* (pp. 25-29).
Qian, M., Wang, J., Sun, S., Song, Z., Yang, S., Wu, Y., Jiang, L., Wang, Q., Dong, K., Xiao, X., Zheng, S., & Chen, G. (2023). Efficacy and safety of endoscopic retrograde cholangiopancreatography in children of pancreaticobiliary maljunction without obvious biliary dilatation. *Journal of Pediatric Surgery*. https://doi.org/10.1016/j.jpedsurg.2023.11.026
Reinhart, W. H., Näf, G., & Werth, B. (2010). Viscosity of human bile sampled from the common bile duct. *Clinical Hemorheology and Microcirculation*, *44*(3), 177–182. https://doi.org/10.3233/ch-2010-1272
Saida, Y. (1992). Clinical and experimental evaluations of bile viscosity in the gallbladder. relation of the viscosity and starvation. *The Japanese Journal of Gastroenterological*

Surgery, *25*(8), 2129–2138. https://doi.org/10.5833/jjgs.25.2129
Sherifi, F., Bexheti, S., Gashi, Z., Bajraktari, I. H., Shatri, J., & Lahu, A. (2018). Anatomic variations of pancreaticobiliary union. *Open Access Macedonian Journal of Medical Sciences*, *6*(6), 988–991. https://doi.org/10.3889/oamjms.2018.196
Shoda, J., Ueda, T., Ikegami, T., Matsuzaki, Y., Satoh, S., Kano, M., Matsuura, K., & Tanaka, N. (1997). Increased biliary group II phospholipase A2 and altered gallbladder bile in patients with multiple cholesterol stones. *Gastroenterology*, *112*(6), 2036–2047. https://doi.org/10.1053/gast.1997.v112.pm9178697
Tajikawa, T., Aoki, K., & Fukuzawa, H. (2023). Investigation of pancreatic juice reflux mechanism in high confluence of pancreaticobiliary ducts and pancreaticobiliary maljunction (Development and validation of a mathematical model for pancreatic and bile juice flow based on fluid mechanics). *Journal of Biorheology*, *37*(2), 44–55. https://doi.org/10.17106/jbr.37.44

Tympner, F., & Rösch, W. (1978). Viscosity of pure pancreatic juice in chronic pancreatitis. *Klinische Wochenschrift*, *56*(8), 421–422. https://doi.org/10.1007/bf01477298 Urushihara, N., Hamada, Y., Kamisawa, T., Fujii, H., Koshinaga, T., Morotomi, Y., Saito, T., Itoi, T., Kaneko, K., Fukuzawa, H., & Ando, H. (2017). Classification of pancreaticobiliary maljunction and clinical features in children. *Journal of Hepato-biliary-pancreatic Sciences*, *24*(8), 449–455. https://doi.org/10.1002/jhbp.485 Von Ritter, C., Niemeyer, A., Lange, V., Möhrle, W., Richter, W., Von Meyer, L., Brandl, H., Del Pozo, R., & Jüngst, D. (1993). Indomethacin decreases viscosity of gallbladder bile in patients with cholesterol gallstone disease. *The Clinical Investigator*, *71*(11). https://doi.org/10.1007/bf00185606
Wang, Q., Moon, S., Zang, J., Liu, J., Weng, H., Wang, X., Wang, J., & Chen, J. (2020). Usefulness of pre‐operative endoscopic retrograde cholangiopancreatography in diagnosis and management of forme fruste choledochal cyst in children. *ANZ Journal of Surgery (Print)*, *90*(6), 1041–1045. https://doi.org/10.1111/ans.15674
Weng, M., Wang, L., Weng, H., Gu, J., & Wang, X. (2021). Utility of endoscopic retrograde cholangiopancreatography in infant patients with conservational endoscopy. *Translational Pediatrics (Print)*, *10*(10), 2506–2513. https://doi.org/10.21037/tp-21-406
Zeng, J., Deng, Z., Yang, K., Zhang, T., Wang, W., Ji, J., Hu, Y., Che, X., & Gong, B. (2019). Endoscopic retrograde cholangiopancreatography in children with symptomatic pancreaticobiliary maljunction: A retrospective multicenter study. *World Journal of Gastroenterology*, *25*(40), 6107–6115. https://doi.org/10.3748/wjg.v25.i40.6107
Zheng, J., Bie, L., Tang, Y., Ge, L., Shen, S., Xu, B., Li, T., & Gong, B. (2017). Endoscopic therapy for patients with pancreaticobiliary maljunction: a follow-up study. *Oncotarget*, *8*(27), 44860–44869. https://doi.org/10.18632/oncotarget.16228 Zyromski, N. J. (2014). *Handbook of Hepato-pancreato-biliary Surgery*. LWW.

Appendix

Appendix Table 1.

Dynamic viscosity of pancreaticobiliary fluids

#	Source	Method	Places of Condition T, ℃	Number of samples	V m

			capture		
1	Kimura,1904, as cited in Li et al., 2007	n.d.	n.d. n.d. n.d.	n.d	1
2	Joel, 1921, as cited in Li et al., 2007	n.d.	n.d. n.d. n.d.	n.d	1
3	Tera, 1960, as cited in Li et al., 2007	Capillary tube with length 8 cm, and diameter 0.2 cm	gallbladder n.d. n.d.	n.d.	2.
4	Bouchier, 1965	Cannon-Manni ng semi-micro viscometer	hepatic gallstone/ 38 (t-tube) normal gallbladder gallstone 38	16 13 of them with gallston es 31	0. 0. ±

normal 38 11 1.93 ± 1.10
47

5	Cowie and Sutor, 1975	Cannon-Fiske capillary viscometer	gallbladder gallstone room temperature	25	12
			common gallstone room bile duct temperature (puncture)	28	1.

6	Tympner and Rosch, 1978	Capillary viscometer	pancreatic juice	normal n.d.	20
				chronic n.d.	20
7	Harada et al., 1981	Cornemicrovisco meter	(papilla of Vater)	pancreatitis	86
8	Okazaki et al.,1986	Microviscosimeter EXlOO	pancreatic juice (papilla of Vater)	chronic n.d.	10
				pancreatitis	11
			pancreatic main duct	normal n.d.	
				chronic n.d.	
				pancreatitis	
9	Gottschalk M and Lochner A, 1990 as cited in Li, 2021	Contraves Low-Shear-Visco meter	hepatic (t-tube)	disease n.d.	33
				(n.d.)	33
10	Saida, 1992	Cone-plate viscometer	gallbladder	normal 37	15
				(gastric cancer)	

11	von Ritter et al., 1993	Contraves Low-Shear-Visco meter	gallbladder	gallstone n.d.	20
				gallstone + indomethacin n.d.	8

			treatment		
12 13	Coene et al., 1994 Shoda et al., 1997	Contraves Low-Shear-Visco meter Automatic Capillary Viscometer	common malignant bile 37 bile duct duct (drainage) obstruction gallbladder adenomatous 37 polyps or normal (gastric cancer) gallstone (solitary cholesterol) gallstone (multiple cholesterol) gallstone (multiple pigment)	14 19 20 24 18	2. 1 2. 3. 6. 3.

14	Jungst et al., 2001	Contraves Low-Shear-Visco meter	gallbladder gallstone 37 (cholesterol stones) gallstone (mixed stones) hepatic gallstone (t-tube)	28 8 6	5. 0. ± 0.

	Ooi, 2004, as cited in Li et al., 2008	n.d.	gallbladder gallstone n.d.	59	1
	6 Gründel et al., 2009	Contraves Low-Shear-Vis co meter	gallbladder gallstone 47	35	0.
17	Reinhart et al., 2010	Contraves Low-Shear-Vis co meter	common bile duct (papilla of Vater) Mixed: gallstone, sludge, cholangitis, a tumour of the head of the pancreas, cholangiocarcinoma, normal. 37	138	0. me 0. me
18	Kuchumov et al., 2014	Physica MCR 501, cone–plate rheometer	hepatic (t-tube) gallstone 37	40	0.

50

19	Kim and Hong, 2020	Automated scanning capillary tube viscometer Hemovister	gallbladder adenoma polyp cholesterol polyp 37	10	5.
				96	1

*Reference for conversion from relative viscosity is distilled water at the temperature of 20℃ [1.0016 mPa], of 38℃ [0.678 mPa]

Appendix Table 2

Carreau models of human bile juice

Source	Li et al.,2008	Kuchumov et al.,2014 Kuchumov et al.,2014

Type of bile Zero shear rate viscosity [μ_0]	Duct bile 10 mPa × s	Duct bile Gallbladder bile 42.8 mPa × s 62.5 mPa × s
Infinite shear rate viscosity [μ] ∞	1 mPa × s	1.3 mPa × s 4.5 mPa × s
Time constant [λ]	160.5742 s	0.04 s 0.033 s
Power index [*a*]	0.4843	0.5 0.56

Equation 51 $\mu = \mu_\infty + (\mu_0 - \mu_\infty)(1 + \lambda^2 \dot{\gamma}^2)^{(a-1)/2}$

Appendix Table 3

Casson-Papanastasiou models of human bile juice

Source	Saida,1992	Kuchumov et al.,2014 Kuchumov et al.,2014
Type of bile	Gallbladder bile	Duct bile Gallbladder bile
Plastic viscosity [$\mu_{◆◆}$]	2.63 ± 0.68 mPa × s	1.2 mPa × s 4.5 mPa × s
Yield stress [τ]$_0$	0.2 ± 0.1 mPa	0.9 Pa 1.68 Pa
Equation	$\mu = (\mu_{◆◆} + \frac{\tau_0}{\dot{\gamma}}[1 - ◆◆◆◆◆◆(- ◆◆\dot{\gamma}^2)])$	